TUHH

Technische Universität Hamburg-Harburg

Institute of River and Coastal Engineering

Modelling of Hydraulic Structures in Hydrodynamic Fluvial Models

Master Thesis

Examiners: Prof. Dr.-Ing. E. Pasche

Prof. Dr.-Ing. W. Schneider

Supervisor: Dipl.-Ing. W. Plöger

Written by

Lu Fang

Matriculation No.: 31554

Submitting date: 11th Jan. 2007

Hamburg, Germany

Abstract

With the improvement of computational capacity and mathematical technique, various multi-dimensional hydrodynamic flow models have been developed and applied to rivers, estuaries and lakes. For many problems, a two-dimensional model would produce considerably satisfactory results. However, when hydraulic structures like weirs, bridges and gates are concerned, the application of normal flow equations can lead to significant deviation due to the change of flow regime around the structure. This can be solved by utilizing three-dimensional models. Nevertheless, three-dimensional models would be in general too expensive, and the detailed flow information around the structure is normally not required. Therefore, the method of modelling hydraulic structures in two-dimensional hydrodynamic fluvial models is analysed in this master thesis.

RMA-10S, which is based on finite element method, is taken as the simulation program. The original assignment within this thesis was to develop the whole mathematical concept for modelling the hydraulic structures in the program. Since it is realized after further analysis that the function of simulating hydraulic structures is already available in RMA-10S, the main task has been adjusted to understand, test and modify this function. The computational logic is explained in this work. Necessary adaptations were also made to integrate the Kalypao-2D models (which were used and developed before at the Institute of River and Coastal Engineering, Hamburg University of Technology) into RMA-10S. The existing function and the corresponding modifications have been tested and verified by extensive models. Adequately satisfactory results have been shown according to the verification. In addition, theories about mathematical modelling and hydraulic structures have also been introduced in this master thesis.

Acknowledgement

The work was carried out within the scope of my master thesis at the Institute of River and Coastal Engineering, Hamburg University of Technology. I would like to express my gratitude to all who gave me the possibility and support to complete this thesis, so that I can finish the thesis despite of the emerged difficulties and unfamiliarity of the mathematical techniques.

It is acknowledged that this master thesis is done by a self-based research work with help of those literatures listed in the reference list.

Lu Fang

11th Jan. 2007
Hamburg, Germany

Contents

Table of Figures

List of symbols

Most of the symbols used in the master thesis are explained here. Some of them may be used in various circumstances. Therefore, their notations also changed according to different contexts.

$[K^e]$	- coefficient matrix / stiffness matrix
$[Q^e]$	- heat generation matrix
$[q^e]$	- heat flux matrix
$[T^e]$	- temperature matrix
A	- two-dimensional ares [m^2]
b	- weir length normal to the flow [m]
c	- heat capacity [J/K]
C	- discharge coefficient for free flow [$m^{1/2}$/s]
c_j	- the value at node j
C_{sub}	- submergence coefficient [-]
D	- a differential operator
$F(x)$	- function to be integrated
$F(x_I)$	- function at the quadrature point x_I
$f_i(u_j^n)$	- residual error with the estimated value u_j^n
$\vec{F}$	- weight forces vector [N]
F_x	- weight forces in x direction
F_y	- weight forces in y direction
h	- water depth at upstream around the weir [m]
H_1	- total head uptream around the weir [m]
h_c	- convective heat conduction coefficient [W/K]
k	- thermal conductivity [W/(Km)]
L	- weir width (total embankment width) in the direction of flow [m]
L_P	- width of the weir crest [m]
m	- mass per unit volume [kg]
N	- a row vector of quadratic basis functions
p	- hydrostatic pressure [N/m2]
$\vec{P}$	- pressure and friction forces vector [N]
q	- internal heat generation [W]
Q	- discharge [m3]
	heat generation per volume unit [W]
q_c	- convective heat conduction [W]
q_n	- heat flux orthogonal to the boundary [W]
$R(x)$	- residual
t	- time [s]
	water depth at downstream around the weir [m]
T	- temperature [K]
T_c	- reference temperature [K]
u	- example of an exact solution
	velocity component in x direction [m/s]
U	- velocity in the flow direction [m/s]
u_0	- value at the start of the time interval
u_j^n	- estimated value at the end of the nth iteration
u_N	- approximated solution

v	- velocity component in y direction [m/s]
$\vec{v}$	- velocity vector [m/s]
V	- volume [m^3]
V_I	- mean velocity at upstream around the weir [m/s]
v_T	- eddy viscosity [Pa·s]
w	- velocity component in z direction [m/s]
w_i	- weighting function
W_I	- quadrature weight
Γ	- boundary
δ_{ij}	- Kronecker unit vector [-]
κ	- turbulent kinetic energy per unit volume [N/m^2]
μ	- coefficient for free flow (DU BUAT, POLENI, WEISBACH formulas) [-]
	- viscosity of the fluid [Pa·s]
ρ	- fluid density [kg/m^3]
σ_{ij}	- total stress [N/m^2]
τ_{ij}	- viscous stress [N/m^2]
φ_j	- approximation function
Ω	- two-dimensional integration area
Φ	- viscous dissipation [W]
ϑ	- numerical integration
$(\frac{\partial f_i}{\partial u_j})_{u^n}$	- derivative evaluated with all the nth estimates of u

1. Introduction

Hydraulic phenomena are complex to describe due to structural multiplicity and complicated interdependency of parameters. Therefore, powerful and reliable instruments are desired to analyse multidimensional flow systems. Numerous scientific researches have improved the understanding of flow mechanics significantly in engineering practice. A variety of mathematical methods, starting with simple, one-dimensional analytical models, up to multi-dimensional numeric models with sophisticated turbulence modelling, have been developed. (Institute of River and Coastal Engineering, 2006) This master thesis introduces one of the numerical modelling programs developed from the seventies, and focuses on the function of simulating hydraulic structures in two-dimensional models.

1.1. History of the hydraulic model RMA-10S

Over the last seventeen years the development and testing of a series of models for simulating estuaries, lakes and rivers have been sponsored by the United States Army Corps of Engineers. In the earliest development phase, two-dimensional models were developed both for laterally averaged and depth averaged approximations. These early studies developed a methodology for solution and simulation of the time dependent, non-linear equations that are typical and used as basis for these problems. (King, 1993) In 1973 RMA-2 (Resource Management Associates) was delivered, and subsequent enhancements have been carried out by King and Roig at the University of California, Davis. RMA-2 is applicable for two-dimensional depth averaged hydrodynamic flow simulation. It utilizes finite element method to compute water levels and horizontal velocity components for both steady and dynamic flow. (Ploeger, 2004)

With the development of computational facilities, the capacity and efficiency of the two-dimensional simulation systems improved significantly. Nevertheless, there are many issues associated with estuaries, rivers and lakes that incorporate stratified three-dimensional flow regimes. The need for three-dimensional simulations has been acknowledged. On the basis of this demand, RMA-10 was developed, which enables the meaningful three-dimensional simulations at a reasonable expense. However, in many problems the area, where a real three-dimensional regime is needed, is often limited, and in a large part of the system two or even one-dimensional approximation would be adequate. Extensive additions to RMA-10 were made that allows coupling of one- and two-dimensional elements and permits the user to select the order of approximation at various locations of the model based upon the actual geometry and expected flow characteristics. Furthermore, water properties (salinity and temperature) can also be simulated by this model. (King, 1993)

RMA-10S is a revised version of RMA-10 which designed to extend the capability of RMA-10 to simultaneous simulation of sand or cohesive sediment transport, including erosion, deposition and tracking of the bed. RMA-10S is taken by the Institute of River and Coastal Engineering at Hamburg University of Technology, and integrated together with its own hydraulic model Kalypso-2D for further modelling researches.

Kalypso-2D originates from RMA-2, and experienced a continuous further development and adjustment by the Institute of River and Coastal Engineering. It applies the graphic interface BCE2D, which was brought to market by Bjoernsen Beratende Ingenieure in Koblenz, Germany. The graphic interface is implemented to the CAD software Microstation. (Ploeger, 2004) While the RMA series uses RMAGEN (a program for generation of finite element networks) and RMAPLT (a program for displaying results from RMA) as graphic interface. The integration of RMA-10S and Kalypso-2D as well as the further development of RMA-10S is one of the research areas at the institute.

Until now RMA-10S is able to read and write the geometry input file for Kalypso-2D models. In addition, the calculation of the flow resistance with Darcy-Weisbach-Equation, which was originally only available in Kalypso-2D, was also implemented in RMA-10S. The resistance depending on vegetation can be now optionally calculated by RMA-10S. (Schrage, 2006)

1.2. Objectives and structure of the thesis

The flow in rivers is often controlled by hydraulic structures such as weirs, bridges and gates. Due to the pressure flow and the change of flow regime within the structure, it is not adequate to describe the hydraulic phenomena around the structure by normal two-dimensional flow equations. The simple application of flow equations may lead to a considerable underestimation of the upstream water elevation around hydraulic structures, which further influences the downstream water elevation and discharge at the hydraulic structures. Although the model quality can be improved by using the three-dimensional simulation around the structures, coupled two- and three-dimensional models would be too expensive for normal engineering problems. (Pasche) The objective of this master thesis is to analyse the modelling of hydraulic structures by two-dimensional flow models.

Within the scope of this thesis, hydraulic structures as well as their control effect on running water should be defined and described. A theoretical concept and its implementation for modelling these structures in two-dimensional finite element models should be developed. A real application should be demonstrated to validate the implemented function.

Mathematical modelling concepts for two-dimensional models and the overall flow chart of RMA-10S are introduced in the next chapter. Theories about hydraulic structures are explained in chapter 4. Numerical concept and its implementation to simulate these structures are discussed in chapter 5, which is followed by verification of the concept using some testing models. Conclusions and further remarks are mentioned in the last chapter.

2. Mathematical modelling concepts for 2D models

There are two major tasks involved in order to studying physical phenomena (Reddy, 1993):

- Mathematical formulation of the physical process
- Numerical analysis of the mathematical model

Development of the mathematical description of a process is achieved through assumptions concerning how the process works. This mathematical description is then transformed into a mathematical model and results are derived by a numerical method.

In this chapter, the governing equations which are used for two-dimensional flows are firstly described, followed by an introduction to Finite Element Method, a variational technique of solving differential equations. This brief introduction outlines the process of moving from a general differential equation to a mathematical solution. The last part of this chapter depicts the overall structure of RMA-10S.

2.1. Governing equations

RMA-10S is able not only to describe stratified flow in three-dimensions, but also to simulate sediment transport simultaneously. The governing equations involve velocity in all three Cartesian directions, water pressure and the distribution of salinity, temperature or suspended sediment as well as sediment transport throughout the system. Therefore, 7 degrees of freedom can be considered and calculated by RMA-10S. These are: water depth, flow velocity in *x*, *y* and *z* directions, temperature, salt and sediment concentration. In this thesis, only equations regarding to two-dimensional flow calculation are considered, thus flow velocity in *x* and *y* directions and water depth are of major importance. A short description of the equations is demonstrated as follows.

The basic hydrodynamic equations for two-dimensional flow models are based on the depth-averaged shallow water equations which assume hydrostatic pressure over the water depth and neglectable vertical components of the flow velocity (Pasche). The governing equations are derived from 3 global laws:

- Continuity equation (conservation of mass)
- Momentum equation (conservation of momentum)
- Energy equation (conservation of energy)

2.1.1. Continuity equation

The continuity equation states that the sum of mass flowing in and out of a volume unit per time is equal to the change of mass per time divided by the change of density (Zienkiewicz and Taylor, 2000). Considering that the volume does not change, it can be expressed as:

$$\frac{D\rho}{Dt}+\left(\frac{\partial(\rho u)}{\partial x}+\frac{\partial(\rho v)}{\partial y}+\frac{\partial(\rho w)}{\partial z}\right)=0 \tag{2.1}$$

For incompressible and isotropic fluid, we assume that the derivatives of the density over time and over Cartesian coordinate system are zero. The result of the continuity equation for ideal fluid can be then written as:

$$\frac{\partial u}{\partial x}+\frac{\partial v}{\partial y}+\frac{\partial w}{\partial z}=0 \tag{2.2}$$

If only considers two-dimensional, the above equation can be simplified as:

$$\frac{\partial u}{\partial x}+\frac{\partial v}{\partial y}=0 \tag{2.3}$$

2.1.2 Momentum equation

The momentum equation is a basic law of mechanics, which states that mass times acceleration is equal to the sum of forces that act on a volume unit. If we differentiate mass forces $\vec{F}$ (weight forces) and surface forces $\vec{P}$ (pressure and friction forces), conservation of momentum can be expressed as (Institute of River and Coastal Engineering, 2006):

$$\frac{1}{dV}\frac{d(m\vec{v})}{dt}=\rho\frac{D\vec{v}}{Dt}=\vec{F}+\vec{P} \tag{2.4}$$

For two-dimensional systems, equation 2.4 can be written as:

$$\begin{aligned}\rho(\frac{\partial u}{\partial t}+u\frac{\partial u}{\partial x}+v\frac{\partial u}{\partial y})&=\frac{\partial \sigma_{xx}}{\partial x}+\frac{\partial \sigma_{xy}}{\partial y}+F_x\\ \rho(\frac{\partial v}{\partial t}+u\frac{\partial v}{\partial x}+v\frac{\partial v}{\partial y})&=\frac{\partial \sigma_{yy}}{\partial y}+\frac{\partial \sigma_{xy}}{\partial x}+F_y\end{aligned} \tag{2.5}$$

The mass forces can be seen as outside forces, in contrast with surface forces which depend on the deformation state of the fluid. In order to further develop the above equation, the connection between the stress state and the deformation state has to be analysed. The total stress σ can be expressed in terms of the viscous stress τ and the hydrostatic pressure p. (Further information can be taken from Reddy, 1993)

$$\sigma_{xx}=\tau_{xx}-p, \qquad \sigma_{yy}=\tau_{yy}-p, \qquad \sigma_{xy}=\tau_{xy} \tag{2.6}$$

The first index of σ and τ stands for the axis that the area element is orthogonal to, the second index for the direction which the stress is pointing to.

The functional relationship between τ_{ij} and the velocity gradient is assumed to be linear and is independent from a rotation of the coordinate system and the change of the axis (isotropy). It yields:

$$\tau_{xx} = \mu(\frac{\partial u}{\partial x} + \frac{\partial u}{\partial x}), \quad \tau_{yy} = \mu(\frac{\partial v}{\partial y} + \frac{\partial v}{\partial y}), \quad \tau_{xy} = \mu(\frac{\partial u}{\partial y} + \frac{\partial v}{\partial x}) \tag{2.7}$$

where μ is the viscosity of the fluid

Substitution of equation 2.5 and 2.6 into 2.4 yields:

$$\begin{aligned} \rho(\frac{\partial u}{\partial t} + u\frac{\partial u}{\partial x} + v\frac{\partial u}{\partial y}) &= \mu(\frac{\partial}{\partial x}(2\frac{\partial u}{\partial x}) + \frac{\partial}{\partial y}(\frac{\partial v}{\partial x} + \frac{\partial u}{\partial y})) - \frac{\partial p}{\partial x} + F_x \\ \rho(\frac{\partial v}{\partial t} + u\frac{\partial v}{\partial x} + v\frac{\partial v}{\partial y}) &= \mu(\frac{\partial}{\partial y}(2\frac{\partial v}{\partial y}) + \frac{\partial}{\partial x}(\frac{\partial v}{\partial x} + \frac{\partial u}{\partial y})) - \frac{\partial p}{\partial y} + F_y \end{aligned} \tag{2.8}$$

The three-dimensional momentum differential equations are known as Navier-Stokes equations. When they are depth-averaged to two-dimensional flow equations, they are called Shallow Water Equations. If the viscosity is zero, they can be simplified as:

$$\begin{aligned} \rho(\frac{\partial u}{\partial t} + u\frac{\partial u}{\partial x} + v\frac{\partial u}{\partial y}) &= -\frac{\partial p}{\partial x} + F_x \\ \rho(\frac{\partial v}{\partial t} + u\frac{\partial v}{\partial x} + v\frac{\partial v}{\partial y}) &= -\frac{\partial p}{\partial y} + F_y \end{aligned} \tag{2.9}$$

which are called Euler equations.

2.1.3. Energy equation

Energy transfer can take place by convection and conduction. The equation of energy conservation can be then expressed as (Reddy, 1993):

$$\rho c(\frac{\partial T}{\partial t} + u\frac{\partial T}{\partial x} + v\frac{\partial T}{\partial y}) = k(\frac{\partial^2 T}{\partial x^2} + \frac{\partial^2 T}{\partial y^2}) + q + \Phi \qquad (2.10)$$

where c is the mean heat capacity at constant volume, q is the internal heat generation, k is the thermal conductivity of the isotropic fluid, and Φ is the viscous dissipation, which is zero for nonviscous fluids. For fluids of low viscosity and for velocities less than the sonic velocity, Φ has a magnitude that is very small compared with the other terms in the equation 2.10.

In summary, the governing equations of two-dimensional flows of viscous incompressible fluids are (2.3), (2.8) and (2.10).

In reality, we differentiate between a laminar and a turbulent flow state. If the flow velocity exceeds a certain boundary value, the flow is turbulent; otherwise it is laminar. Although turbulence is a very complex phenomenon characterized by chaotic and stochastic property changes, it is still possible to use the general Navier-Stokes equations in consideration of the random fluctuation of velocity. The most frequently used approach is to average the momentum equation with respect to time. This approach is based on the assumption that the turbulent velocity fluctuations are distributed stochastically, meaning there is a constant mean flow velocity. This averaging leads to the so-called Reynolds Averaged Navier-Stokes equation. More detailed information is demonstrated in relevant literature (e.g. Lecture Notes: Environmental Hydraulic Simulation by Institute of River and Coastal Engineering, 2006). Only the result of the general time-averaged Navier-Stokes equations, also called Reynolds equations, is illustrated here in tensor form:

$$\rho(\frac{Du_i}{Dt}) = F_i - \frac{\partial p}{\partial x_i} + \frac{\partial}{\partial x_j}\tau_{ij} \qquad (2.11)$$

with $\tau_{ij} = \mu\frac{\partial u_i}{\partial x_j} + \rho(v_T(\frac{\partial u_i}{\partial x_j} + \frac{\partial u_j}{\partial x_i}) - \frac{2}{3}\kappa\delta_{ij}$

where κ is the turbulent kinetic energy, δ_{ij} is Kronecker unit vector (δ_{ij}=1 for i=j, δ_{ij}=0 for $i \neq j$), and v_T is the eddy viscosity, which can be calculated by turbulence models.

In most two-dimensional cases, the mixing process and flow structure are not influencing each other that the flow equations and the advection / diffusion – equation can be solved independently. However, in case of density stratification, flow equations and the advection / diffusion equation have to be solved simultaneously. (Pasche) The governing equations for three-dimensional stratified flow in RMA-10S are slightly different from the equations explained here. It includes the momentum equations in three directions, continuity equation, advection / diffusion equation and the equation of state.

2.2. Finite Element Method

The governing equations have to be solved by numerical methods. The Finite Element Method (FEM) is used in RMA-10S for solving differential equations and integrals. The most distinctive feature of FEM which separates it from others is the division of a given domain into a set of simple sub-domains, called finite elements. Any geometric shape that allows computing the solution or its approximation, or provides necessary relations among the values of the solution at selected points (called nodes) is regarded as a finite element. (Reddy, 1993)

The finite element method is a computational technique used to obtain approximate solutions of boundary value problems in engineering (Hutton, 2004). It is based on the idea that the solution u of a differential equation can be approximated by a linear combination of the parameter c_j and the appropriate functions φ_j.

$$u \approx u_N = \sum_{j=1}^{N} c_j \varphi_j(x) \tag{2.12}$$

where u is the exact solution and u_N is the approximated solution, the c_j is the value at the node j, and φ_j is the so-called approximation or interpolation function, which satisfies the boundary conditions.

In order to solve the equation, the approximation functions have to be determined. There are various variational methods of approximation, for example the Rayleich-Ritz method and method of weighted residuals. While the latter can be further distinguished into Galerkin method, the least square method etc (Institute of River and Coastal Engineering, 2006). A brief introduction of weighted residuals method will be illustrated later in this chapter.

The major steps to analyse and solve the problem by using FEM are as follows (Institute of River and Coastal Engineering, 2006):

(1.) Discretization of the domain into a set of finite elements.

(2.) Derivation of the weighted residual integral or the weak form of the governing differential equations to investigate and implement the finite element approach

(3.) Assembly the elements in a global, algebraic system of equations

(4.) Applying boundary conditions to the system of equations

(5.) Solving the equations

(6.) Formatting or visualizing the solution

2.2.1. Method of Weighted Residuals

The method of weighted residuals (MWR) is an approximate technique for solving boundary value problems that constructs approximation function satisfies prescribed boundary conditions and an integral formulation to minimize error in an average sense over the problem domain. The approximation functions φ_j should be continuous over the whole domain and satisfy the specified boundary conditions exactly. Furthermore, it should also satisfy the "physics" of the problem in a general sense. Given all these conditions, it is unlikely that the solution represented in equation 2.12 is exact. A residual error therefore results (Hutton, 2004):

$$R(x) = D[u_n(x), x] \neq 0 \qquad (2.13)$$

where *R(x)* is the residual and *D* is a differential operator.

The residual is also a function of the unknown parameter c_j. With the help of the method of weighted residuals, the parameters c_j are chosen so that the residual *R* approaches zero. Considering a two-dimensional problem, this requirement can be expressed as (Institute of River and Coastal Engineering, 2006):

$$\int_{\Omega} w_i(x, y) R(x, y, c_j) dxdy = 0 \qquad i=1,2,\ldots\ldots,n \qquad (2.14)$$

where $w_i(x,y)$ represent n arbitrary weighting functions. The integration is over the two-dimensional area Ω.

Equation 2.14 results in n algebraic equations, which can be solved for the n values of c_j. Since the boundary conditions must be satisfied, the solution is exact at the end points. However, in general the residual error is nonzero at any interior point. The MWR may capture the exact solution under certain conditions, but it is an exception rather than the rule.

There are several variations of MWR which vary primarily in how the weighting functions are determined or selected. The most common techniques are point collocation, sub-domain collocation, least squares, and Galerkin method. These methods mainly differ in the choice of the weighting function and the approximation function. The Galerkin method is used in the finite element form of the depth-averaged shallow water equation, since it is quite simple to use and readily adaptable to the finite element method. It assumes that the weighting function is identical to the approximation function.

$$\int_{\Omega} w_i(x,y)R(x,y,c_j)dxdy = \int_{\Omega} c_i(x,y)R(x,y,c_j)dxdy \tag{2.15}$$

2.2.2. The Weak Form

A weak form is a weighted-integral statement of a differential equation in which the differentiation is distributed among the dependent variable and the weighting function. It includes also the natural boundary conditions of the problem (Reddy, 1993). A simple example is used here to demonstrate how a weak form is derived. The example is the steady temperature distribution $T(x,y)$ in a two-dimensional isotropic medium Ω with the boundary Γ. (Institute of River and Coastal Engineering, 2006) It can be stated as:

$$-\left\{\frac{\partial}{\partial x}\left(k\frac{\partial T}{\partial x}\right)+\frac{\partial}{\partial y}\left(k\frac{\partial T}{\partial y}\right)\right\}=Q \qquad \text{in } \Omega \tag{2.16}$$

where k is the heat conduction coefficient in x and y direction and $Q(x,y)$ is the provided heat generation per volume unit (source term).

The following boundary conditions are defined prior to solving the differential equation 2.16.

$$T = \hat{T}(s) \qquad \text{on the boundary } \Gamma_T \tag{2.17}$$

$$(k\frac{\partial T}{\partial x}n_x + k\frac{\partial T}{\partial y}n_y) + q_c = q(s) \qquad \text{on the boundary } \Gamma_q \tag{2.18}$$

The boundaries Γ_T and Γ_q do not overlap, and s is the coordinate along the boundary line, (n_x,n_y) is the unit vector normal to the boundary and q_c is the convective heat conduction defined by:

$$q_c = h_c\,(s,T)\,(T - T_c) \tag{2.19}$$

where h_c is the convective heat conduction coefficient and T_c is the reference temperature. The finite element approximation can be expressed as:

$$T(x,y) \approx T^e(x,y) = \sum_{j=1}^{n} T_j^e w_j^e(x,y) \tag{2.20}$$

There are three steps to develop the weak form of any differential equation:

Step 1. All expressions of the differential equation are moved to one side, the entire equation is multiplied with a weighting function w, and integrate over the domain Ω of the problem.

$$0 = \int_{\Omega^e} w\left\{-\frac{\partial}{\partial x}(k\frac{\partial T}{\partial x}) - \frac{\partial}{\partial y}(k\frac{\partial T}{\partial y}) - Q\right\}dxdy \tag{2.21}$$

Step 2. After transferring the differentiation of the variable into the weighting function in the first step, the differentiation is equally distributed between u and w, and the component form of the gradient (or divergence) theorem is recalled on the boundary.

Step 3. The actual boundary conditions of the problem are imposed on the weak formulation under consideration.

The interim transformation steps are avoided here, the weak form of this example can be finally written as:

$$0 = \int (k \frac{\partial w}{\partial x} \frac{\partial T}{\partial x} + k \frac{\partial w}{\partial y} \frac{\partial T}{\partial y} - wQ) dxdy - \oint_{\Gamma^e} w q_n ds \tag{2.22}$$

where q_n is the heat flux orthogonal to the boundary, which can also be described as:

$$q_n = k \frac{\partial T}{\partial x} n_x + k \frac{\partial T}{\partial y} n_y \tag{2.23}$$

In order to transfer the weak form into a finite element form, the finite element approximation for *T* (equation 2.20) is substituted into equation 2.23. After several modifications, this equation can be written in matrix form:

$$[K^e]\{T^e\} = \{Q^e\} + \{q^e\} \tag{2.24}$$

with

$$K_{ij}^e = \int_{\Omega^e} (k \frac{\partial w_i^e}{\partial x} \frac{\partial w_j^e}{\partial x} + k \frac{\partial w_i^e}{\partial y} \frac{\partial w_j^e}{\partial y}) dxdy \tag{2.25}$$

The matrix $[K^e]$ is the coefficient matrix, also called stiffness matrix in statistics.

2.2.3. The approximation functions

For the finite element approximation $T^e(x, y)$ of $T(x, y)$ to converge against the true solution for the element Ω^e in the example above, the approximation functions have to match a few criteria (Reddy, 1993):

(1) They have to be differentiable, as required in the weak form of the problem, meaning that all terms in the weak form are represented as nonzero values.

(2) The polynomials used to make up the approximation function must be complete. It means that all terms of the polynomial starting with the constant to the term of the highest order should be included in the function.
(3) All terms used in the polynomial should be linearly independent.

The detailed steps to derive the approximation functions are not illustrated here. There is large amount of relevant literature regarding to this topic (e.g. Reddy, 1993).

2.2.4. Numerical integration

Integration of various functions of the field variable is required for formulation of finite element coefficient matrices. For example, the Galerkin method requires integration over the element domain (and physical volume), once for each approximation function. Integration is required to obtain the value of every component in the coefficient matrix of a finite element. (Hutton, 2004) Exact evaluation of the integrals appearing in element coefficient matrices and source vectors is not always possible because of the algebraic complexity of the coefficients in differential equations. Numerical evaluation of these integral expressions is therefore demanded. Numerical evaluation of integrals, called numerical integration or numerical quadrature, involves approximation of the integrand by a polynomial of sufficient degree. A quadrature formula has a general form (Reddy, 1993):

$$\vartheta = \int_{x_A}^{x_B} F(x)dx \approx \sum_{I=1}^{r} F(x_I)W_I \qquad (2.26)$$

where x_I are the quadrature points and W_I are the quadrature weights.

The commonly used integration methods can be classified into two groups:

- The Newton-Cotes formula that employs values of the function at equally spaced base (or quadrature) points
- The Gauss quadrature formula that employs unequally spaced base points.

The most popular numerical technique is Gauss (or Gauss-Legendre) quadrature. The detailed description refers to Reddy (1993) or Hutton (2004). The error of the numerical integration can be reduced by either decreasing the element size or increasing the degree of the approximation (the order of the polynomial function). The interpolation functions used for the approximation of the dependent variable are generally different from the approximations for geometry discussed in chapter 2.2.2. Isoparametric approximation, in which the degree of approximation used for both geometry and dependent variables is equal, is used in RMA-10S.

2.2.5. Assembly of element equations

In deriving the element equations, the formulated variational problem of a typical element is isolated from its finite element model. To solve the whole problem, we must put the elements back to their original positions in the matrix. The assembly of finite element equations is based on two principles (Reddy, 1993):

- Continuity of the primary variables at connecting nodes (Primary variable is the dependent unknown in the same form as the weighting function in the boundary expression. Its specification constitutes the essential boundary condition, e.g. temperature for the example in chapter 2.2.2)
- "Equilibrium" (or "balance") of secondary variables at connecting nodes (secondary variable is the coefficient of the weight function in the boundary expression Its specification constitutes the natural boundary condition, e.g. heat conduction for the example in chapter 2.2.2)

Continuity of the primary variables refers to the single valued nature of the solution at connecting nodes, which means the last nodal value of the element Ω^e is the same as the first nodal value of the adjacent element Ω^{e+1}. Balance of secondary variables refers to the equilibrium of point sources at the junction of several elements. The temperature distribution example in 2.2.2 with two elements is used to demonstrate the assembly of element equations:

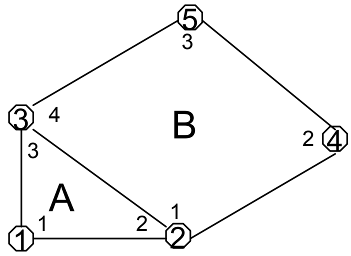

Figure 2.1 Assembly of global equations
(Reddy et al., 1994 cited by Institute of River and Coastal Engineering, 2006)

The equations for the individual elements are:

Element A:

$$
\begin{aligned}
K_{11}^{A}T_{1}^{A} + K_{12}^{A}T_{2}^{A} + K_{13}^{A}T_{3}^{A} &= Q_{1}^{A} + q_{1}^{A} \\
K_{21}^{A}T_{1}^{A} + K_{22}^{A}T_{2}^{A} + K_{23}^{A}T_{3}^{A} &= Q_{2}^{A} + q_{2}^{A} \\
K_{31}^{A}T_{1}^{A} + K_{32}^{A}T_{2}^{A} + K_{33}^{A}T_{3}^{A} &= Q_{3}^{A} + q_{3}^{A}
\end{aligned}
\tag{2.27}
$$

Element B:

$$
\begin{aligned}
K_{11}^{B}T_{1}^{B} + K_{12}^{B}T_{2}^{B} + K_{13}^{B}T_{3}^{B} + K_{14}^{B}T_{4}^{B} &= Q_{1}^{B} + q_{1}^{B} \\
K_{21}^{B}T_{1}^{B} + K_{22}^{B}T_{2}^{B} + K_{23}^{B}T_{3}^{B} + K_{24}^{B}T_{4}^{B} &= Q_{2}^{B} + q_{2}^{B} \\
K_{31}^{B}T_{1}^{B} + K_{32}^{B}T_{2}^{B} + K_{33}^{B}T_{3}^{B} + K_{34}^{B}T_{4}^{B} &= Q_{3}^{B} + q_{3}^{B} \\
K_{41}^{B}T_{1}^{B} + K_{42}^{B}T_{2}^{B} + K_{43}^{B}T_{3}^{B} + K_{44}^{B}T_{4}^{B} &= Q_{4}^{B} + q_{4}^{B}
\end{aligned}
\tag{2.28}
$$

After implementing the principles of the equations system and the boundary conditions, the global system of equations in this example can be written in the following matrix form:

$$
\begin{pmatrix}
K_{11}^{A} & K_{12}^{A} & K_{13}^{A} & 0 & 0 \\
K_{21}^{A} & (K_{22}^{A}+K_{11}^{B}) & (K_{23}^{A}+K_{14}^{B}) & K_{12}^{B} & K_{13}^{B} \\
K_{31}^{A} & (K_{32}^{A}+K_{41}^{B}) & (K_{33}^{A}+K_{44}^{B}) & K_{42}^{B} & K_{43}^{B} \\
0 & K_{21}^{B} & K_{24}^{B} & K_{22}^{B} & K_{23}^{B} \\
0 & K_{31}^{B} & K_{34}^{B} & K_{32}^{B} & K_{33}^{B}
\end{pmatrix}
\begin{pmatrix} T_1 \\ T_2 \\ T_3 \\ T_4 \\ T_5 \end{pmatrix}
=
\begin{pmatrix} Q_{1}^{A} \\ Q_{2}^{A}+Q_{1}^{B} \\ Q_{3}^{A}+Q_{4}^{B} \\ Q_{2}^{B} \\ Q_{3}^{B} \end{pmatrix}
+
\begin{pmatrix} q_{1}^{A} \\ q_{2}^{A}+q_{1}^{B} \\ q_{3}^{A}+q_{4}^{B} \\ q_{2}^{B} \\ q_{3}^{B} \end{pmatrix}
\tag{2.29}
$$

3.2.6. The Newton Raphson Method

The assembled element coefficient matrix (shown by equation 2.29) is nonlinear and asymmetric and must be solved using an iterative method, which seeks an approximate solution to the algebraic equations by linearization (Reddy, 1993). Newton Raphson Method is one of the most common methods for solving nonlinear systems.

It is a successive approximation technique which computes adjustments to an existing estimate of the solution to a set of simultaneous nonlinear equations. Each set of adjustment is called iteration. It seeks to eliminate the residual determined by substituting the estimated solution into the governing equations. The solution is improved by computing the slopes of the residual error functions with respect to each of the unknown variables and carrying out a simultaneous correction of all the estimates assuming the error functions are locally linear. The Newton Raphson method defines a series of corrections Δu_j as (King, 1993):

$$\sum_{j=1}\left(\frac{\partial f_i}{\partial u_j}\right)_{u^n}\Delta u_j + f_i = 0 \qquad \text{for i = 1, N} \tag{2.30}$$

The residual error for equation i computed from estimated values u_j^n at the end of the nth iteration is represented as $f_i(u_j^n)$. If the solution were exact, f_i would then be identical to zero for all i. Assume that there are N equations and N unknown values for u_j^n. $\left(\frac{\partial f_i}{\partial u_j}\right)_{u^n}$ is the derivative evaluated with all the nth estimates of u. The square matrix with elements $\left(\frac{\partial f_i}{\partial u_j}\right)_{u^n}$ is called the Jacobian $[J^n]$ system at nth iteration.

Physically the changes Δu_j are imposed to reduce the calculated error f_i to zero. For linear systems $\left(\frac{\partial f_i}{\partial u_j}\right)_{u^n}$ would be a constant independent of u_j and the adjustment computed by this procedure would lead to the exact solution after one iteration from any starting estimate. For nonlinear problems, the error from the solution of this set of equations is supposed to be reduced with iteration. Although reduction of error is not guaranteed for the method, experience has shown that if the starting estimate is sufficiently close, the reduction in error does occur and the solution method converges. (King, 1993)

Since the model uses an iterative procedure to solve nonlinear equations, it is necessary to define when iteration is complete. RMA-10S uses two criteria to terminate iteration:

- For both the initial steady state and subsequent dynamic iterations a maximal number of allowable iterations is defined.
- Another criterion is convergence tolerance, which can be specified for each active dependent variable used in the simulation. If the maximal absolute value of the change during iteration is less than the specified value for any variable or set of variables, that variable is considered as converged and solution automatically jumps to the next

iteration that involves an unconverged variable. If none is found, the solution is considered converged.

The relaxation parameter, which relieves the value of the change by a factor between 1 and 0, can also be specified during any iteration step.

2.2.7. Time integration

A semi-implicit time solution scheme is implemented in RMA-10S. The objective is to replace the time derivative with a finite difference formulation. The derivation of the scheme is explained briefly as follows. (King, 1993)

An expression of a parameter over a time interval Δt is given by:

$$u = u_0 + at + bt^{\alpha} \tag{2.31}$$

where u_0 is the value at the start of the time interval; a and b are constants to be determined. The first derivative over t is:

$$\frac{\partial u}{\partial t} = a + \alpha b t^{\alpha - 1} \tag{2.32}$$

Let $(\partial u/\partial t)$ at time $t = 0$ be $(\partial u/\partial t)_0$, then $a = (\partial u/\partial t)_0$
This leads to:

$$\left(\frac{\partial u}{\partial t}\right) = \left(\frac{\partial u}{\partial t}\right)_0 + \alpha b t^{\alpha - 1} \tag{2.33}$$

Substituting for b from equation 2.31 and at time Δt this can be re-arranged to become:

$$\left(\frac{\partial u}{\partial t}\right) = (1 - \alpha)\left(\frac{\partial u}{\partial t}\right)_0 + \alpha (u - u_0) / \Delta t \tag{2.34}$$

This form can be entered into the finite element integrals:

$$\int N^T \frac{\partial u}{\partial t} dA = \int N^T \left[(1-\alpha)\left(\frac{\partial u}{\partial t}\right)_0 + \alpha(u-u_0)/\Delta t \right] dA \qquad (2.35)$$

where N is a row vector of quadratic basis functions and represents a succession of geometric functions defined over a nominal element so that it has unit value at one node point and zero at all other node points. It is used for example as the weighting function for the momentum equations.

Equation 2.35 indicates that the time derivative can be expressed as a function of known values at the beginning of the time step and the dependent variable itself. For the Newton Raphson Method we obtain:

$$\frac{\partial}{\partial u}\int N^T \frac{\partial u}{\partial t} dA = \int N^T \frac{\partial}{\Delta t} N dA \qquad (2.36)$$

Equations like 2.36 may be used to substitute for the Jacobians that include time derivatives of each of the dependent variables in the finite element integral equations.

The contribution to the residual error function is the estimated value of *($\partial u/\partial t$)* obtained from equation 2.34. When $\alpha = 1.0$ it is a fully implicit scheme. When $\alpha = 2.0$ a time centred semi-implicit scheme is derived which is identical to the Crank Nicholson scheme (for further information please turn to other finite element literature). In RMA-10S, $\alpha = 1.6$ is used, which corresponds to forward time centring at 62.5% between the new and old time levels (full time centred at 50%). This value is applied for the time derivative in all the governing partial differential equations. Experience suggested that as α tends towards 2.0, the numerical stability decreases. When $\alpha = 1.6$ the numerical damping is still kept to a minimal level. (King, 1993)

2.3. Basic structure of RMA-10S

RMA-10S is programmed in Fortran language to use FEM analysis solving the governing differential equations. The model operates interactively with the user requesting file names for data input. To start a dynamic simulation, a geometry input file and the control file (in which the values of many parameters are entered) are basically required. The general flowchart illustrates the overall flow of data and interaction of the major program parts.

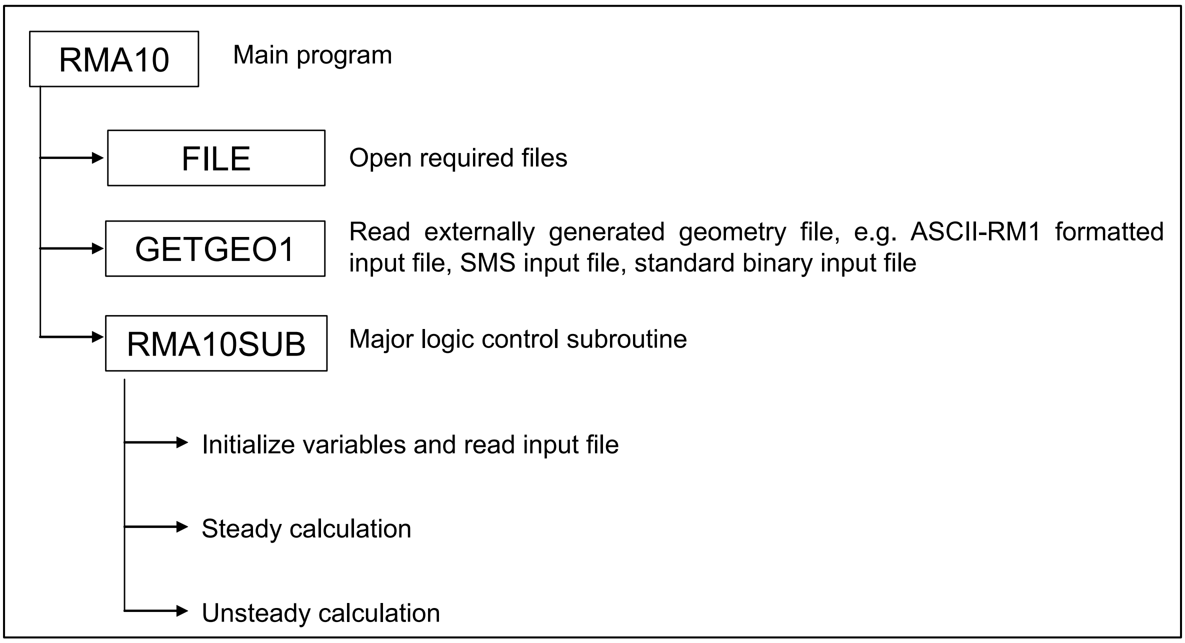

Figure 2.2 Overall flowchart of RMA-10S

The logic of unsteady calculation is the same as steady calculation. The only difference is that the computational logic is within the main dynamic loop for the time steps, and some data are updated at the beginning of the time step loop. The result for the steady simulation or each time step of the unsteady simulation is calculated iteratively by the Newton Raphson Method, until convergence or the maximum iteration number is reached. The computational logic and information flow are illustrated as follows:

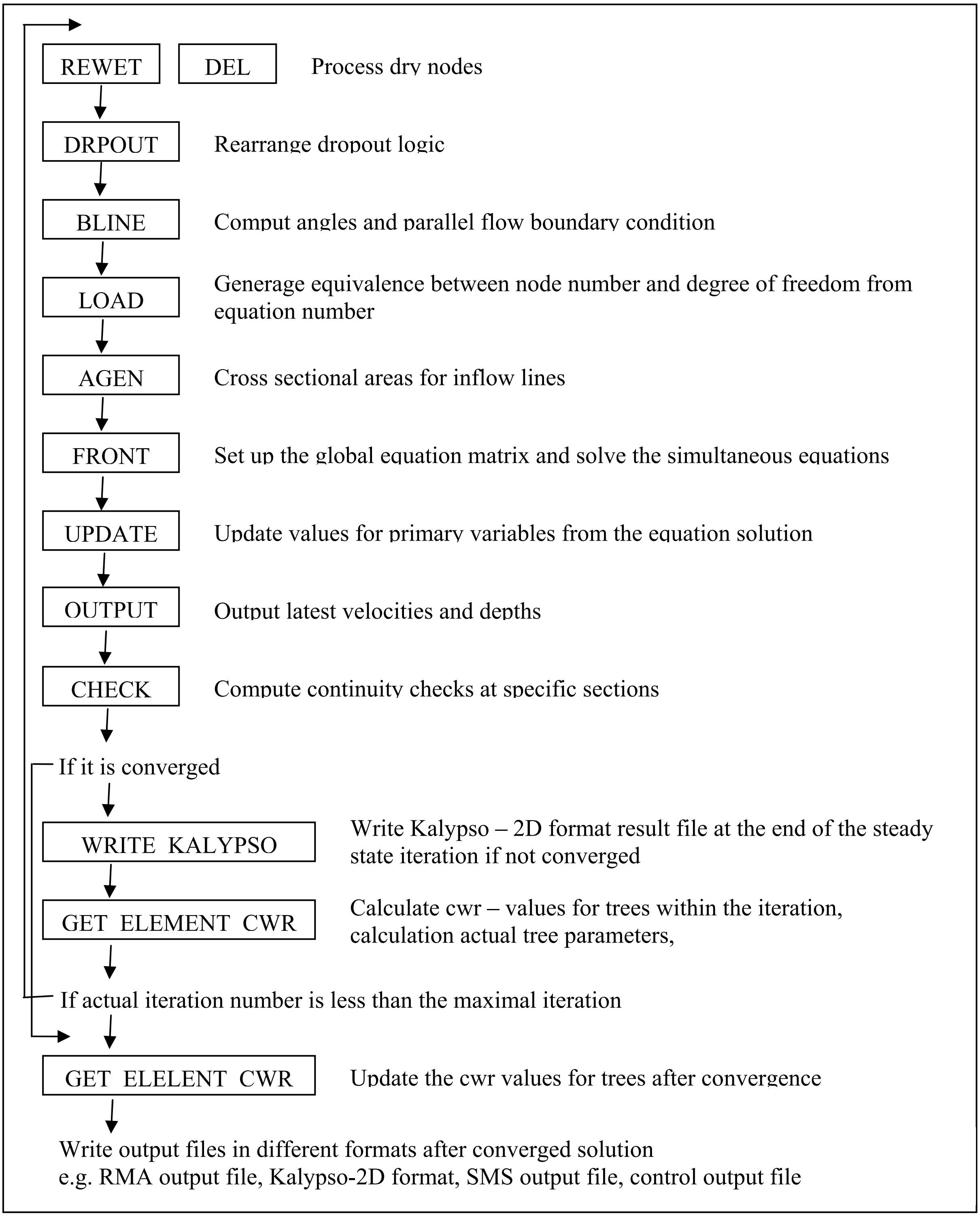

Figure 2.3 Computation logic

(Names in the rectangular framework and written in capital are subroutines.)

3. Theories about hydraulic structures

Hydraulic structures are basically man-made interventions and devices on streams and conduits to measure or regulate flows. They can be made from rocks, concrete, wooden timbers, tree trunks etc. and usually related to irrigation, drainage, water supply, sewage and hydropower projects. Hydraulic structures are classified based on the purpose of the structure in measuring, retention or regulation and discharge types. (Institute of River and Coastal Engineering, 2005) They can be further distinguished as weirs, sluice gates, local obstacles, bridges, outlets, culverts and so on. The variety of structures that can be presented in a stream system is practically unlimited. However, they all include a hydraulic loss, where the deterministic factors are upstream and downstream water elevation and the corresponding discharge. Therefore, for any type of hydraulic structure the most important issue is to describe the relationship between the water level and the discharge. In this master thesis, weir structures have been taken to consider their influence on the flow. A weir can be defined as an obstruction on a channel bottom over which fluid must flow (Munson et al., 1990 cited by Cigana). For weir structures, the theory is developed essentially from the results of experimental tests of flow through the structure for different upstream and downstream flow depths. In the following section, one theory based on the experiments, will be introduced, and this is also implemented in RMA-10S.

3.1. Theory and formulas implemented in RMA-10S

Various studies about weirs are available, and several theories have been developed from them. The formulas implemented in the code are originally from Geological Survey Water-supply Paper “Studies of flow of water over weirs and dams” (Kindsvater, 1964), which illustrates the results from considerable testing experiments.

A weir forms a control section at which the discharge can usually be determined on the basis of a filed survey of water levels and the geometry of the weir structure. Formulas and discharge coefficients are given for three general classes of weirs according to their crest shape: sharp-crested, broad-crested and round-crested. However, many weirs do not neatly fit into these three categories, because of shape, physical condition of the channel, or the hydraulic conditions under which the weirs are operating. For example, a broad-crested weir may act like a sharp-crested weir when the head is sufficient to make the nappe spring clear. It is therefore necessary to consider many different aspects of the situation – shape of weir, geometry of the channel, ratio of head to crest length – before classifying the weir as to the appropriate discharge equation and coefficient. The formulas used in the code are for highway embankment, which becomes a weir when it is overtopped by floods. It is classified as a form of broad-crested weir. The weir is called broad-crested, only if the crest length is so long that influences of curved stream lines on the discharge capacity of the weir are negligible. (Hulsing, 1967)

To analyse flow over various weirs, flow patterns also have to be distinguished. It is classified into two main categories: free and submerged flow. For the low tailwater (downstream) condition, known as free flow, the discharge is determined by the upstream head. At higher tailwater levels, when the depth of flow over the roadway is everywhere greater than the critical depth, the discharge is controlled by the capacity of the tailwater channel as well as the upstream head. The flow is said to be submerged, when tailwater has to be taken into consideration. With a rising tailwater level, the change from free flow to submerged flow occurs rather abruptly. The transition from free flow to submerged flow is described as incipient submergence. In the laboratory test procedure, the tailwater level corresponding to incipient submergence for a given discharge was determined by gradually raising the tailwater and observing the tailwater level at which the headwater (upstream) began to rise. (Kindsvater, 1964)

The discharge equation and coefficients for flow over a highway embankment implemented in RMA-10S are given in this section. The geometry and flow pattern for a highway embankment are illustrated in figure 3.1. Under free-flow conditions critical depths occur near the crown line. The height of the embankment has no influence on the discharge coefficient.

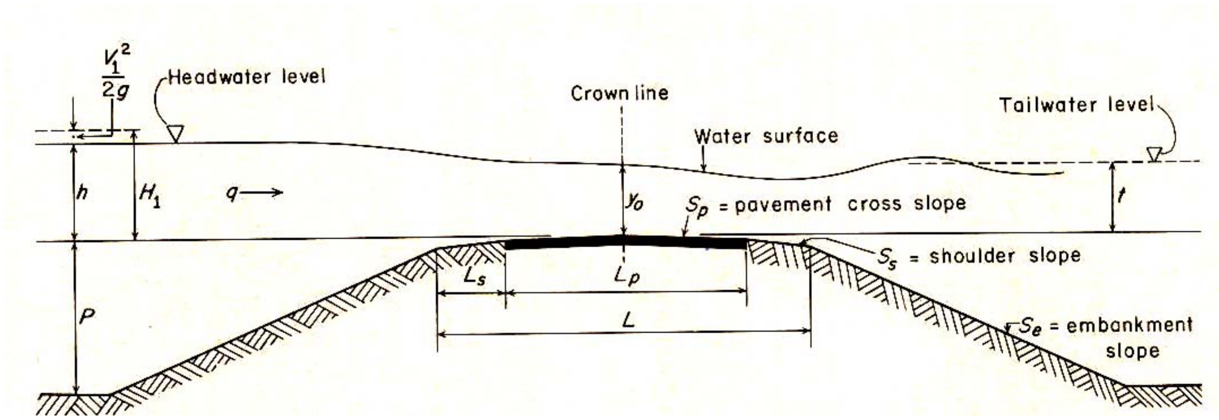

Figure 3.1 Profile of a highway embankment (Kindsvater, 1964, P13)

3.1.1. Free flow

Discharge control occurs at a critical flow section on the roadway for free flow which means that a unique relationship exists between the discharge and the head on the embankment. From the one-dimensional energy and continuity equations for the reach between a section at the crown line and a section in the channel immediately upstream from the embankment, the free discharge equation can be derived as (Kindsvater, 1964):

$$Q = CbH_1^{3/2} \qquad (3.1)$$

where Q: discharge

C: discharge coefficient

b: width of weir crest normal to flow (weir length)

H_1: total head ($h + V_1^2 / 2g$) referred to the crest of the weir, and V_1 is the mean velocity at the approach section to the weir.

Discharge coefficient for free flow

Tests made to determine the coefficient of discharge for free flow involved the measurement of the head and discharge. The discharge coefficient C is then computed from the equation 3.1. Values of C in the test models are plotted as a function of both h and h/L, where h is the piezometric head measured in the model and L is the total width of pavement in the flow direction. The two abscissa scales have independent physical meanings: h is a scale of reference for the influence of boundary resistance and "scale effect", because *h* is directly proportional to Reynolds number; while *h/L* is a scale of reference for form effects, including the effect of curvilinear flow at the control section. The nature of the weir surface (roadway) is distinguished as paved and gravelled according to the roughness. The result is shown in figure 3.2 and 3.3.

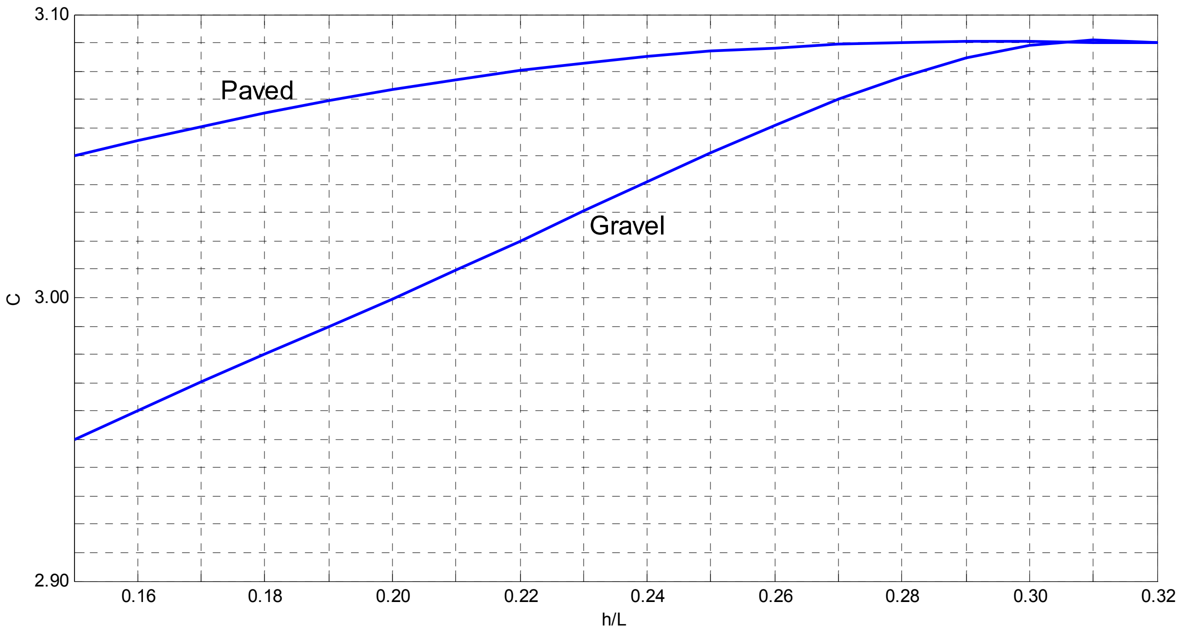

Figure 3.2 Discharge coefficients for highway embankments for *h/L* ratios > 0.15 (Hulsing, 1967, P27)

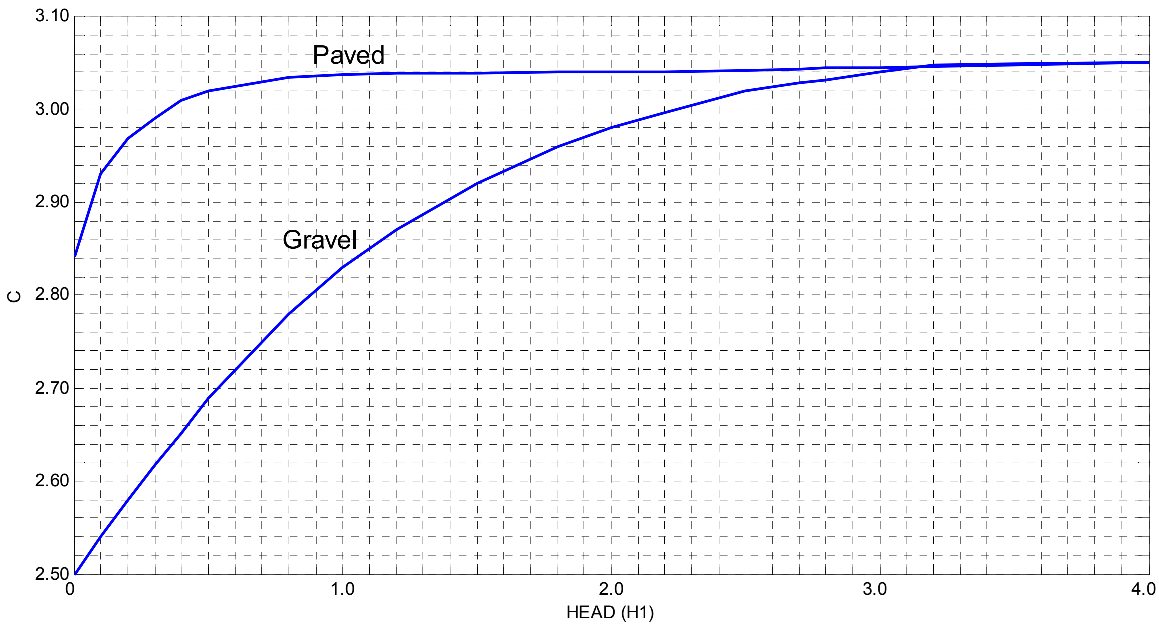

Figure 3.3 Discharge coefficients for highway embankments for *h/L* ratios < 0.15 (Hulsing, 1967, P27)

The discharge coefficient is defined as a function of *h/L* on figure 3.2 for the condition *h/L*>0.15; for the condition *h/L*<0.15 it is defined as a function of head. The upper and lower curve should be used for paved and gravelled highways respectively. (Note: these values are in unit of feet.)

3.1.2. Submerged flow

Equation of discharge for free flow is derived on the basis of a simple energy analysis, considering that the critical flow control occurs on the roadway when the flow is free. However, when the flow is submerged, the discharge capacity of the downstream channel is a primary control. Therefore, for submerged flow, the discharge depends on the tailwater level as well as the total head of headwater. (Kindsvater, 1964)

Discharge coefficient for submerged flow

It is impractical to derive an independent equation for submerged flow. The most expedient alternative is an empirical solution based on experiment and the free-flow discharge equation. The degree of submergence of a highway embankment is defined by the ratio *t/h*. It is also the parameter to distinguish the submerged flow from free flow. The effect of submergence on the discharge coefficient is expressed by the factor C_{sub}. The coefficient of discharge for submerged flow is independently related to all the variables involved in free flow, plus the submergence ratio, *t/h*. The relation of C_{sub} to the degree of submergence for paved and gravel surfaces is illustrated in figure 3.4. In order to virtually eliminate the influence of the embankment height *P*, the submergence ratio is defined as t/H_1 instead of *t/h*. The factor C_{sub} is multiplied by the discharge coefficient for free flow conditions to obtain the discharge coefficient for submerged conditions. (Kindsvater, 1964)

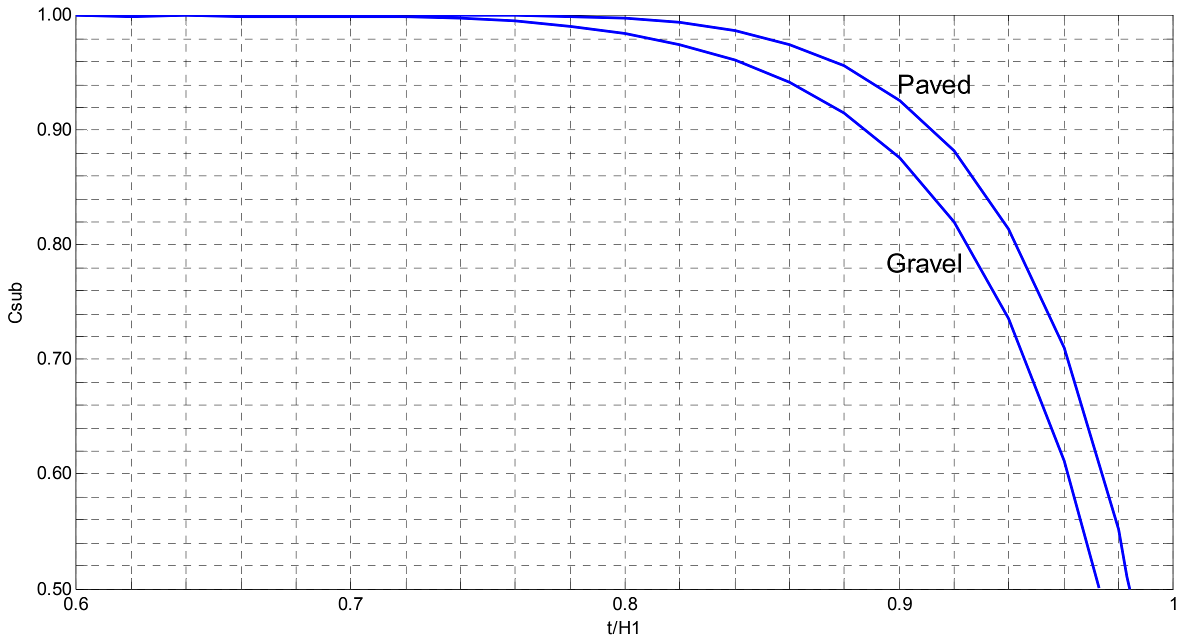

Figure 3.4 Submergence factor for submerged highway embankment
(Hulsing, 1967, P27)

In conclusion, the model tests show that the most significant characteristics of both free and submerged flow are virtually independent of embankment shape and relative height (*h/P*). The discharge coefficient for free flow is primarily a function of head, roadway roughness and the head-width ratio (*h/L*). The discharge coefficient for submerged flow is primarily a function of submergence ratio (t/H_1) and the roughness of the roadway surface. (Kindsvater, 1964)

3.2. Other weir overflow formulas

There are other formulas derived from various theories. In this part, some of them will be introduced briefly. POLENI equation, which is widely applied in Germany, will be explained for further comparison with the weir equation implemented in RMA-10S.

3.2.1. Free overflow

Other most common overflow formulas include DU BUAT, POLENI and WEISBACH. (Institute of River and Coastal Engineering, 2005)

DU BUAT: $Q = \frac{2}{3}\mu b\sqrt{2gH_1^3}$ (3.2)

POLENI: $Q = \frac{2}{3}\mu b\sqrt{2gh^3}$ (3.3)

WEISBACH: $Q = \frac{2}{3}\mu b\sqrt{2g}\left[\left(h + \frac{V_1^2}{2g}\right)^{3/2} - \left(\frac{V_1^2}{2g}\right)^{3/2}\right]$ (3.4)

In order to compare the results calculated by the weir equation 3.1 from the program and other theories, one of the above formulas (POLENI) will be introduced explicitly, especially the discharge coefficient for broad-crested weirs. According to KNAPP, the weir is broad-crested, if the following relation is met (Institute of River and Coastal Engineering, 2005):

$L > 3\, H_1$

However, POLENI equation is true for any shape of weirs. The calculation of the free or submerged flow in Germany is usually done with constant discharge coefficients within the POLENI equation. The values of free flow coefficient μ for various weir shapes are shown in figure 3.5. In the standard guideline of dimensioning sewer and buildings inside the sewer systems in Germany (ATV-A 111, 1994 cited by Peter), a constant μ = 0.5 is given for all weirs except the sharp-crested weir. It is however necessary to validate dynamic coefficients to represent the behaviour of the flows at the weir sites. (Peter)

Shape of the crest		µ
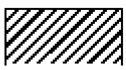	broad-crested weir	0,49-0,51
	broad-crested weir, chamfered	0,50-0,55
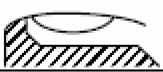	drum gate: perfect round-crested weir	0,65-0,73
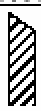	sharp-crested weir with full aeration under the nappe	0,64
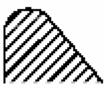	round-crested weir with a slope on the down-stream side	0,75
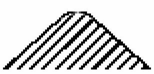	round-crested weir with a slope on both sides	0,79

Figure 3.5 discharge coefficient µ for free flow (Peter, P1)

3.2.2. Subcritical overflow

The overflow is subcritical if the discharge is influenced by a respectively high tailwater level. During the downstream water level rises, the critical overflow becomes subcritical. There are boundary conditions for round-crested weirs that define the transition between critical and subcritical overflow. For broad-crested weirs the free overflow immediately becomes subcritical when the critical depth at the downstream weir side is exceeded. (Institute of River and Coastal Engineering, 2005)

The capacity loss caused by the influence of the downstream water level on the overflow is also considered by multiplying a factor C_{sub} for subcritical overflow. It results in a decrease of the discharge capacity.

$$C_{sub} = \sqrt{1-\left(\frac{t}{h}\right)^{n}} \tag{3.5}$$

where n is the exponent according to different weir crest shapes

broad-crested: $n = 16$

totally round-crested: $n = 10$

pointed: $n = 9.2$

round with perpendicular upperstream-side: $n = 4.9$

sharp-crested: $n = 1.6$

The POLENI equation is used in chapter 5 to compare the result computed in the program.

4. Implementation of hydraulic structures

The original assignment of this master thesis also includes the complete development of a mathematical concept for modelling hydraulic structures in RMA-10S. POLENI formula is firstly defined to be implemented in the source code. However, after a short analysis of the existing program, it is found that the function of simulating weir structures already exists in RMA-10S. Therefore, the major task of this work has been changed to understand the logical concept, test the available functions, debug and integrate the Kalypso 2D models into RMA-10S.

4.1. General concept and overall structure

When the flow in rivers is controlled by structures like weirs, bridges and gates, no hydrostatic pressure distribution over the water depths occurs, due to pressure flow, change of the flow regime and steep water surface gradients within the structure. In some cases, the vertical velocity component is not negligible. The application of the flow equations can lead to a considerable underestimation of the upstream water level of the flow structures. How to consider control structures in the model becomes a practical problem for hydraulic engineers. The interactive dependency of the discharge (velocity) and the downstream and upstream water elevation around the structure is the major difficulty in the simulation model.

The basic logic behind the two-dimensional control structure (e.g. weir) simulation in RMA-10S is to implement weir equation for the weir elements in order to calculate discharge over the weir and the corresponding derivatives according to the water elevations from last iteration. These derivatives from the weir equation and continuity equation are then employed in the global equation matrix and solved simultaneously with other elements and equations. When the weir structure is totally submerged, this function is switched off. The weir elements are considered as normal elements and the Navier-Stokes equations are implemented again. In this case, special consideration of bottom roughness has to be given for weir structures to simulate backwater effect.

There are two schemes available in RMA-10S to derive weir overflow and the derivatives. One is to calculate the discharge over weir structures by calling a subroutine in which the weir equation is implemented; the other is to interpolate the discharge based on the input values in an extra weir input file.

Weir elements, which are defined by giving the element type number (roughness class) between 904 and 989, are firstly tested whether they are submerged. Special boundary conditions should also be considered for weir structures in the relevant subroutine. There is another additional function available by which control structures (e.g. gates) can be switched on and off and the time series can be specified in a text file. All the related subroutines are illustrated in figure 4.1, followed by a short explanation of each subroutine.

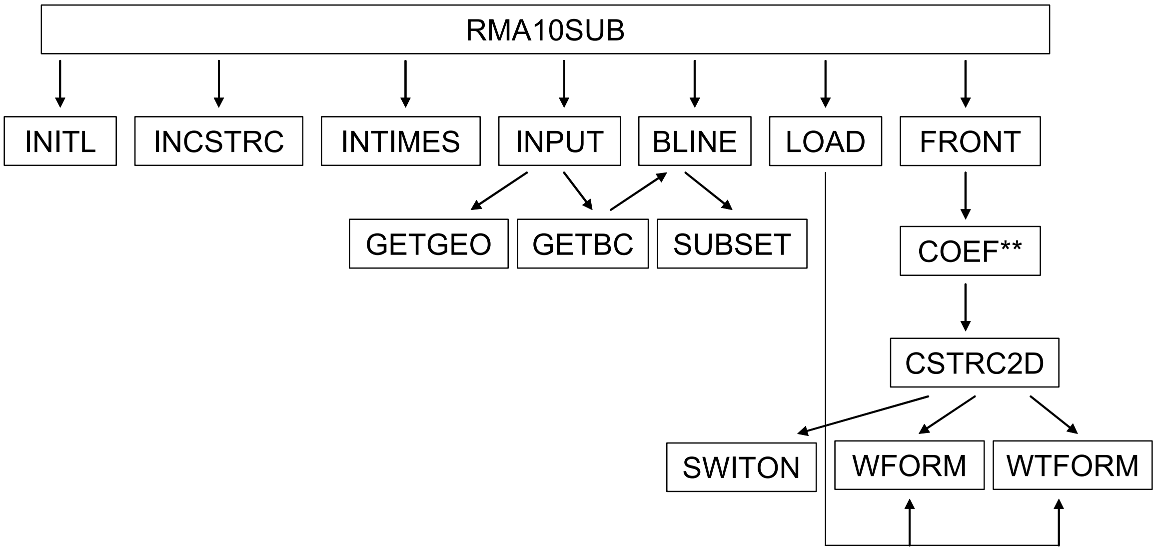

Figure 4.1 Subroutines related to simulation of hydaulic structures

INITL: initialize weir data, set weir elevation and transition elevation to -10000 at every node.

INCSTRC: read the additional weir input file if it exists.

INTIMES: read the weir time switch input file, if it exists.

INPUT: control the inflow of geometrical and control data.

GETGEO: input principal elements of the geometry of the system. Weir data are read from the control file.

GETBC: control and input boundary conditions. Weir structures are specially considered.

BLINE: compute angles and parallel flow boundary conditions. Some commands are used to redirect weir.

SUBSET: test and set whether weir elements are submerged.

LOAD: generate equivalence between node number and degree of freedom from equation number. It also established lists indicating compilation of equation formulation. Hydraulic structures are specially considered.

COEF**: generatge element coefficient matrices. CSTRC2D is called if the weir element is not submerged.

CSTRC2D: generate element coefficient matrices for two-dimensional hydraulic structure elements.

SWITON: determine whether the control structure is switched on or off.

WFORM: compute weir flows.

WTFORM: determine weir flows according to the weir data input file.

4.2. Relevant subroutines

Subroutines closely related to weir structure simulations can be divided into 4 groups based on their functionalities and are analysed below:

- Control of overall information flow: CSTRC2D
- Computation of discharge over weir structures: GETBC, SUBSET and WFORM
- Linear interpolation of discharge among the input values: INCSTRC, WTFORM
- Time series to switch control structures on and off: INTIMES, SWITON

4.2.1. Control of overall information flow

Subroutine CSTRC2D

CSTRC2D is the main control subroutine for hydraulic control structures, calling from COEF** only if the weir element is not submerged. Various subroutines are called in CSTRC2D to compute or interpolate the weir overflow. The calculated derivatives of discharge over water depth are then transferred in the global coefficient matrix in FRONT.

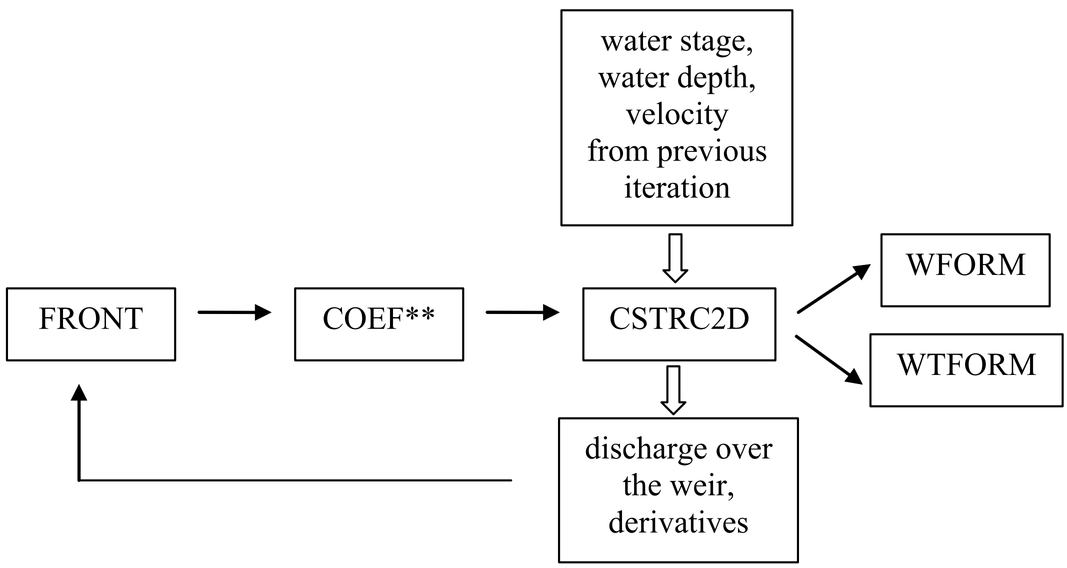

Figure 4.2 Information flow for weir structures

There are two equations considered in this subroutine for weir elements: continuity equation and weir overflow equation (water stage and discharge relationship). These two equations are only considered for the three pair of nodes upstream and downstream (node 1, 2, 3, 5, 6, and 7) at the weir element. The water depth of the mid-side nodes (node 2 and 6 in figure 4.3) are taken by the average value of the two adjacent corner nodes.

Continuity equation: $fu_1 = Q_{source} + h_{upstream} U_{upstream} - h_{downstream} U_{downstream}$ (4.1)

with $Q_{source} = 0$ in the source code, and U is velocity in the direction of flow.

Weir equation: $fu_2 = QW - Q$ (4.2)

with QW calculated in WFORM or interpolated in WTFORM for the weir overflow at corner nodes, at mid-side node $QW = \frac{U_1 h_1 + U_3 h_3}{4} + \frac{U_5 h_5 + U_7 h_7}{4}$

$$Q = \frac{1}{2}\left(h_{upstream} U_{upstream} + h_{downstream} U_{downstream}\right)$$

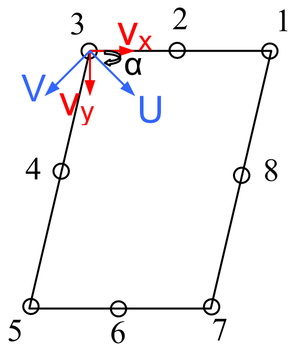

Figure 4.3 An example of a weir element

Velocities in *x* and *y* directions are projected in the flow direction *U* according to the nodal boundary slope *α*. The nodal boundary slope *α* is defined normally in subroutine BFORM by the angle of velocity in *x* and *y* directions, which can also be specified externally in the control file at BN or SN lines for special case. The nodal boundary slope *α* can also be read by GETGEO from binary or ASCII geometry file, or set to the specified values individually at SL lines in the control file to over-ride the calculated nodal boundary slope values. In this case, velocity *V* is eliminated from the coefficient matrix. Therefore, although it is a two-dimensional element, the upstream and downstream water depth *h* and velocity *U* relationship is set only regarding to the corresponding two nodes for each equation, similar as one-dimensional element. Only the change of velocity *U* is calculated by the Newton Raphson Method for weir elements. The change of water depth *h* at the node is derived at the neighbouring element, and is not considered in the local matrix for weir elements. Taking all these elimination results into account, the 24*24 dimensional (8 nodes * 3 degrees of freedom) matrix is simplified into 12*12 (6 nodes * 2 degrees of freedom, velocity V should be all the time zero). The matrix $[J]\{\Delta U\}=\{F\}$ is illustrated below.

$$
\begin{pmatrix}
\frac{\partial fu_{11}}{\partial U_1} & \frac{\partial fu_{11}}{\partial h_1} & \frac{\partial fu_{11}}{\partial U_2} & \frac{\partial fu_{11}}{\partial h_2} & \cdots & \frac{\partial fu_{11}}{\partial U_7} & \frac{\partial fu_{11}}{\partial h_7} \\
0 & 0 & 0 & 0 & \cdots & 0 & 0 \\
\frac{\partial fu_{12}}{\partial U_1} & \cdots\cdots & & & & & \\
0 & \cdots\cdots & & & & & \\
\frac{\partial fu_{13}}{\partial U_1} & \cdots\cdots & & & & & \\
0 & \cdots\cdots & & & & & \\
\frac{\partial fu_{25}}{\partial U_1} & \cdots\cdots & & & & & \\
0 & \cdots\cdots & & & & & \\
\frac{\partial fu_{26}}{\partial U_1} & \cdots\cdots & & & & & \\
0 & \cdots\cdots & & & & & \\
\frac{\partial fu_{27}}{\partial U_1} & \cdots\cdots & & & & & \\
0 & \cdots\cdots & & & & &
\end{pmatrix}
\begin{pmatrix}
\Delta U_1 \\ \Delta h_1 \\ \Delta U_2 \\ \Delta h_2 \\ \Delta U_3 \\ \Delta h_3 \\ \Delta U_5 \\ \Delta h_5 \\ \Delta U_6 \\ \Delta h_6 \\ \Delta U_7 \\ \Delta h_7
\end{pmatrix}
=
\begin{pmatrix}
-h_1U_1 + h_7U_7 \\
0 \\
-\frac{(h_1+h_3)U_2}{2} + \frac{(h_5+h_7)U_6}{2} \\
0 \\
-h_3U_3 + h_5U_5 \\
0 \\
Q-QW \\
0 \\
Q-QW \\
0 \\
Q-QW \\
0
\end{pmatrix}
\qquad (4.3)
$$

$\frac{\partial fu_{ij}}{\partial U_j}$: i refers to the type of equation, whether it is continuity or weir equation; j stands for the node number. Each non-zero coefficient in the matrix is listed as follows.

$\frac{\partial fu_{11}}{\partial U_1} = h_1$, $\frac{\partial fu_{11}}{\partial h_1} = U_1$, $\frac{\partial fu_{11}}{\partial U_7} = -h_7$, $\frac{\partial fu_{11}}{\partial h_7} = -U_7$,

$\frac{\partial fu_{12}}{\partial h_1} = \frac{U_2}{2}$, $\frac{\partial fu_{12}}{\partial U_2} = \frac{h_1+h_3}{2}$, $\frac{\partial fu_{12}}{\partial h_3} = \frac{U_2}{2}$,

$\frac{\partial fu_{12}}{\partial h_5} = -\frac{U_6}{2}$, $\frac{\partial fu_{12}}{\partial U_2} = -\frac{h_5+h_7}{2}$, $\frac{\partial fu_{12}}{\partial h_6} = -\frac{U_6}{2}$,

$\frac{\partial fu_{13}}{\partial U_3} = h_3$, $\frac{\partial fu_{13}}{\partial h_3} = U_3$, $\frac{\partial fu_{13}}{\partial U_5} = -h_5$, $\frac{\partial fu_{13}}{\partial h_5} = -U_5$,

$$\frac{\partial fu_{25}}{\partial U_3} = -\frac{h_3}{2}, \qquad \frac{\partial fu_{25}}{\partial h_3} = -\frac{U_3}{2} + \frac{\Delta QW}{\Delta h_3}, \frac{\partial fu_{25}}{\partial U_5} = -\frac{h_5}{2}, \qquad \frac{\partial fu_{25}}{\partial h_5} = -\frac{U_5}{2} + \frac{\Delta QW}{\Delta h_5}$$

$$\frac{\partial fu_{26}}{\partial U_1} = \frac{h_1}{4}, \qquad \frac{\partial fu_{26}}{\partial h_1} = -\frac{U_1 + U_2}{4}, \quad \frac{\partial fu_{26}}{\partial U_2} = -\frac{h_1 + h_3}{4},$$

$$\frac{\partial fu_{26}}{\partial U_3} = \frac{h_3}{4}, \qquad \frac{\partial fu_{26}}{\partial h_3} = -\frac{U_2 + U_3}{4}, \quad \frac{\partial fu_{26}}{\partial U_5} = \frac{h_5}{4}, \qquad \frac{\partial fu_{26}}{\partial h_5} = -\frac{U_5 + U_6}{4}$$

$$\frac{\partial fu_{26}}{\partial U_6} = -\frac{h_5 + h_7}{4}, \quad \frac{\partial fu_{26}}{\partial U_7} = \frac{h_7}{4}, \qquad \frac{\partial fu_{26}}{\partial h_7} = -\frac{U_6 + U_7}{4}$$

$$\frac{\partial fu_{27}}{\partial U_1} = -\frac{h_1}{2}, \qquad \frac{\partial fu_{27}}{\partial h_1} = -\frac{U_1}{2} + \frac{\Delta QW}{\Delta h_1}, \frac{\partial fu_{27}}{\partial U_7} = -\frac{h_7}{2}, \frac{\partial fu_{27}}{\partial h_7} = -\frac{U_7}{2} + \frac{\Delta QW}{\Delta h_7}$$

The change of discharge with regard to the change of water depth $\frac{\Delta QW}{\Delta h_j}$ is computed by calling subroutine WFORM or WTFORM several times. Each time with $\frac{\Delta h_j}{2}$ increase or decrease to the water depth h_j at node j as input to calculate the new discharge QW. These coefficients are brought to global matrix and the derivatives of velocities and water depth are solved simultaneously with other elements.

CSTRC2D is only for two-dimensional weir structures and the defined weir elements can only be quadrangular with 8 nodes (including mid-side nodes). Weir elements are identified by given the element type between 904 and 989. There are several different functions available for various hydraulic structure types. Type 10 for weir structures is currently in use.

The weir overflow is either calculated or interpolated per unit width to account for the possibility that the weir crest is not horizontal. Brater and King (1976, cited by Franz and Melching, 2004) demonstrated that the equation resulting from the integration of the unit-width weir equation gives a close approximation to the flow for a triangular, sharp-crested weir (V-notch weir). The weir crest is assumed to vary linearly between adjacent nodes. For each line segment (upstream or downstream for each weir element), the flow per unit width is considered at three points: two corner nodes and a mid-side node. The velocity is computed for each node and results in the unit width of flow over the weir at this node alone. This differs from the typical practice for weir overflows where a homogenous velocity across the whole weir section is used, and the total overflow is considered. As the velocity is not constant along the weir crest and may vary from node to node, it gives a more realistic representation of the flow field approaching the weir than the constant-velocity approximation. (Franz and Melching, 2004)

The change of discharge over the weir corresponding to the little change of water depths at each node is calculated. It is then used as the derivative of discharge over water depth in the subroutine FRONT. Weir equation and continuity equation as well as other equations (e.g. for checking the elevation relationship at mid-side nodes) are then used as the governing equations for the further simulation. This is how the weir structure is considered in the whole model.

The flowchart of subroutine CSTRC2D for weirs (type 10) is demonstrated as follows.

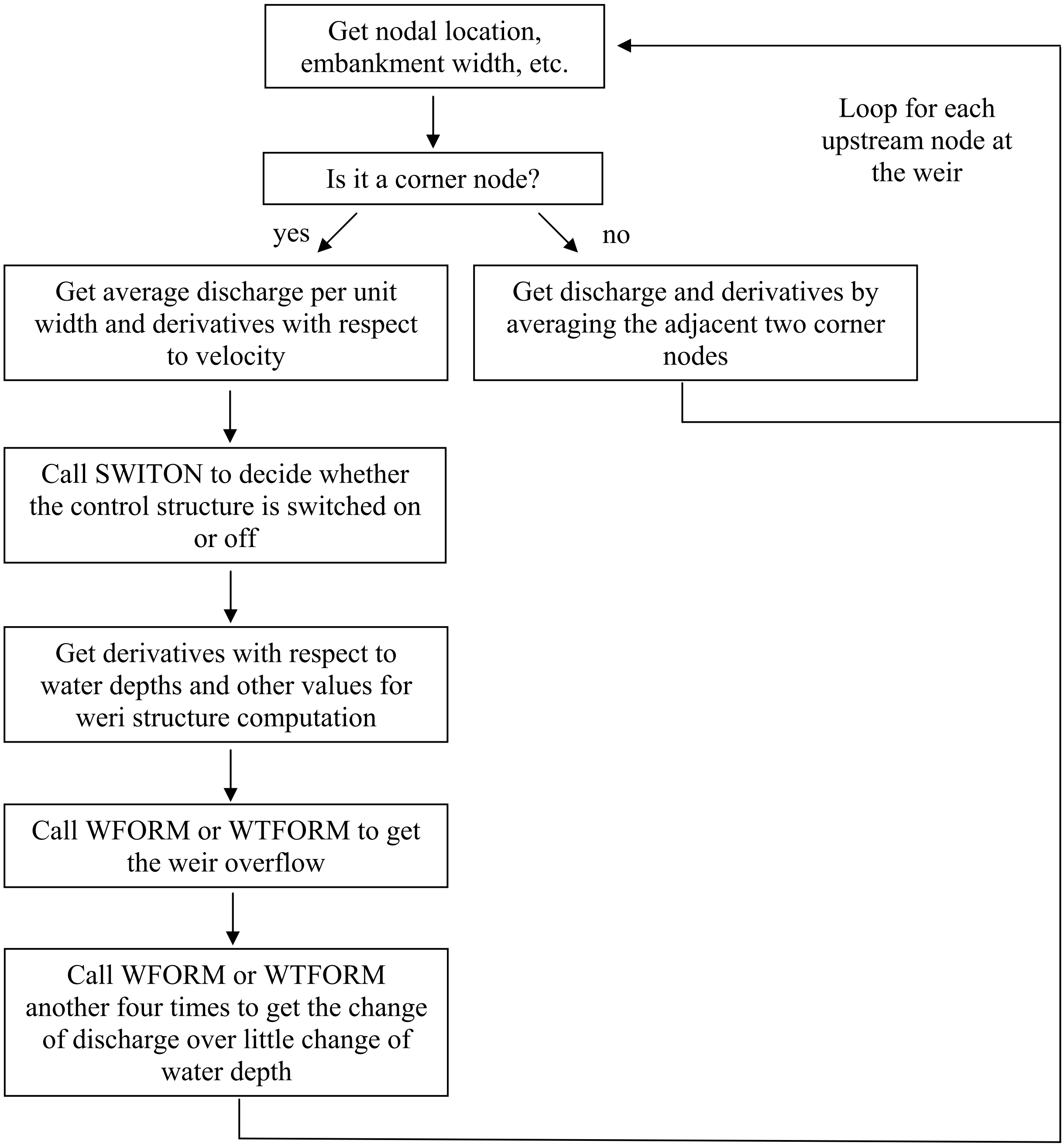

Figure 4.4 Flowchart of subroutine CSTRC2D

According to the theory introduced in chapter 3.1, the elevation of the weir crest, the width of the crest in the direction of flow, and the nature of the crest surface (paved or gravelled) must be specified by the user. However, the nature of the crest surface is presumed to be paved in RMA-10S due to historical reasons. In addition to other two parameters, the transition elevation should also be input into the program. However, this transition elevation is not the same as the transition elevation between the free and submerged flow. It is the transition elevation, above which the earlier defined weir elements should be regarded as normal elements. In this case, weir equation is not used any more.

4.2.2. Computation of discharge over weir structures

Subroutine GETBC

Its general function is to control and input boundary conditions for the whole program. In this subroutine, weir data, which are input at “WDT” lines in the control file and read by GETGEO, are distributed to each node around weir elements if they are only defined at downstream or upstream at the structure. Mid-side nodes obtain the average value of the adjacent two corner nodes. The input weir height is then tested whether it is less than 0.1 m higher than the bottom elevation. If it is, one warning message will appear in the simulation window, but the simulation process is not affected. It is only meaningful for weir discharge computation, when weir data (crest elevation, weir width in the flow direction and transition elevation) have to be entered in the control file specified by the line ID “WDT”.

Subroutine SUBSET

If a weir element is submerged, it is treated later as a normal element. Check of the weir elements’ submergence is fulfilled by subroutine SUBSET. It is only done for the first iteration at each time step. For the rest of the iterations within one time step, the value of submergence parameters, which define whether a node or element is submerged, remains the same. Two arrays are used to decide whether a weir element is submerged: ISUBM (index: node number) and ISUBMEL (index: element number). They are the submergence parameters referring to each node and each element respectively. Additional weir data are demanded as input at “WDT” lines in the control file to define whether the weir element is submerged. These include weir crest elevation and transition elevation for nodes at the weir structure. The procedure to test and set the submergence parameters are illustrated below.

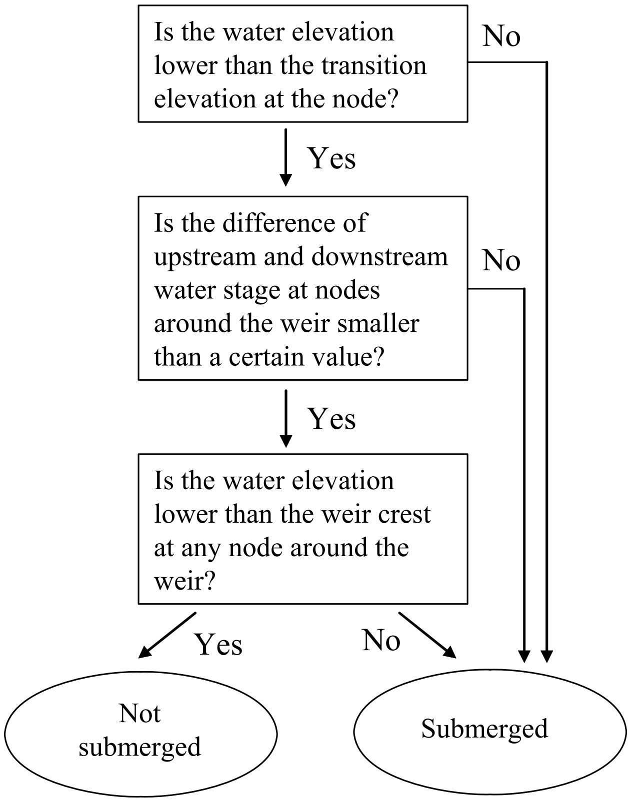

Figure 4.5 Submergence test

Results of the submergence test store in the two arrays. The values of the element array are set according to the array for nodes based on the submergence test. Values of the two variables can be:

ISUBM (node):

-1: initial value

0: not submerged, or initial value for nodal boundary conditions

1: submerged

2: nodal boundary conditions for the first iteration, or submerged at previous iteration but not submerged at actual iteration.

ISUBMEL (element):

0: initial value, or not submerged

1: submerged

The most important outcome of this subroutine is the value of ISUBMEL. Subroutine CSTRC2D is only called when the weir element is not submerged which means that ISUBMEL equals zero. One remark should be made at this point. According to the submergence test, if water elevations at all the corner nodes are higher than the weir crest height, the weir element is submerged and subroutine CSTRC2D is not called. The backwater effect is only calculated by giving a corresponding roughness coefficient (e.g. Manning coefficient). It should be, however, more plausible to consider backwater effect by using weir equations when the water depth over the weir is very shallow (just above the weir crest). It would be more reasonable just to use the input transition elevation as the criterion to judge whether the backwater effect should be calculated by weir equations. The illustrated submergence test procedure would be simplified only according to the input transition elevation.

At the end of the subroutine, two comments can be written in the output file: either the element submerged or the element is flowing. Therefore, the general outcome of the subroutine (the result of the submergence test) can also be check.
Submerged: if water elevations at all corner nodes around the weir element are higher than weir crest.
Flowing: if any of the corner nodes around a weir element has a higher water elevation than the weir crest but not all of them.

Subroutine WFORM

Formulas introduced in chapter 3.1 are generally implemented in this subroutine. Coefficients in the equations are assumed to be interpolated from the figures. Nevertheless, there are still some discrepancies in the code compared to the theory introduced in chapter 3.1. For example, the distinguished parameter between low and high head is upstream head divided by weir crest width (H_1/L_P) in the code, instead of upstream water depth divided by weir width (h/L). Weir overflow depends on the upstream (headwater) and downstream (tailwater) water elevation around the weir structure. It is therefore important to define the upstream and downstream at the weir. In this subroutine, direction of flow is firstly tested and set according to upstream and downstream weir water elevation from the last iteration. After initializing the parameters, weir calculation is carried out following several conditions, which is mainly illustrated in the figure below. The free flow coefficient is firstly calculated, and then submergence coefficient is computed if necessary, at last the discharge over the weir is calculated per unit width ($q = CH_1^{3/2}$). Although the computation scheme includes both paved and gravelled surface roughness as discussed in chapter 3.1, it is presumed that the weir highroad surface is paved in the source code.

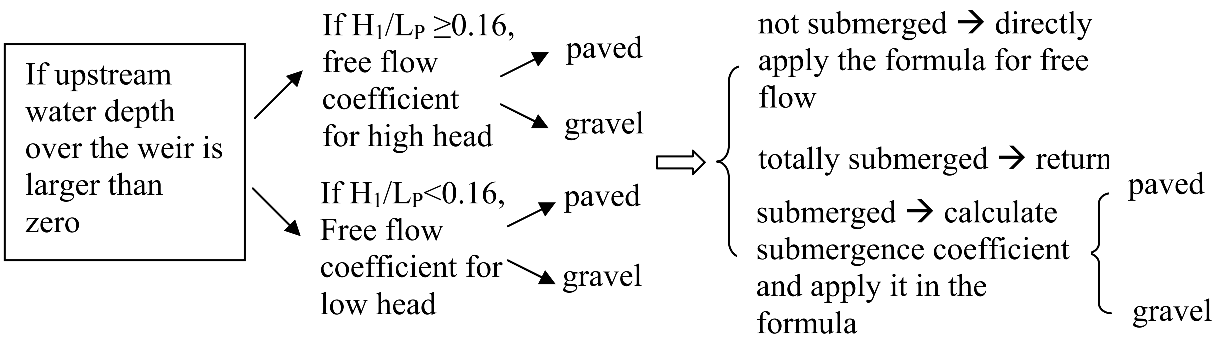

Figure 4.6 Flowchart of weir overflow calculation

The general formula is the same as introduced in chapter 3.1: $Q = C \times C_{sub} \times H_1^{3/2}$, but only unit width discharge is computed for each node. Exact formulas to determine the coefficients are explained below.

<u>Discharge coefficient *C* for free flow:</u>

$H_1/L_P < 0.16$

$$\text{paved} \begin{cases} H_1 < 0.1,\ C = 1.59 + H_1 \times 0.8 \\ H_1 < 0.9,\ C = 1.67 \\ H_1 < 1.2,\ C = 1.67 + \dfrac{(H_1 - 0.9) \times 0.2}{3} \\ \text{else},\ C = 1.69 \end{cases} \tag{4.4}$$

$$\text{gravel} \begin{cases} H_1 < 0.9,\ C = 1.38 + 0.3\sqrt{H_1} \\ H1 < 1.2,\ C = 1.67 + \dfrac{(H_1 - 0.9) \times 0.2}{3} \\ \text{else},\ C = 1.69 \end{cases} \tag{4.5}$$

$H_1/L_P \geq 0.16$

$$\text{Paved:} \quad C = 1.686 + 0.05\sqrt{\frac{H_1}{L_P} - 0.16} \tag{4.6}$$

$$\text{gravel}\begin{cases} H_1 < 0.288,\ C = 1.634 + 0.07 \times \dfrac{H_1}{L_P} \times \dfrac{1}{0.128} \\ \text{else},\ C = 1.686 + 0.05\sqrt{\dfrac{H_1}{L_P} - 0.16} \end{cases} \tag{4.7}$$

Discharge coefficient C_{sub} for submerged flow:

$t/H_1 < 0.76$

$$C_{sub} = 1.9 \times \left(\frac{H_1}{L_P}\right)^{0.22} - 0.28 \tag{4.8}$$

$t/H_1 \geq 0.76$

$$\text{paved: } C_{sub} = 1 - 0.65\left(\frac{t/H_1 - 0.76}{0.24}\right)^4 \tag{4.9}$$

$$\text{gravel: } C_{sub} = 1 - 0.8\left(\frac{t/H_1 - 0.76}{0.24}\right)^3 \tag{4.10}$$

The implemented formulas are slightly different from the theory in chapter 3.1. However, the general concept is similar. L_P is the width of the crest, which defines flow over the roadway. Hulsing (1967) indicated that L_P is difficult to define and recommended that five-sixths of the maximum piezometric head be used to define the level that establishes the limits of flow.

4.2.3. Linear interpolation of discharge

Subroutine INCSTRC

Subroutine INCSTRC reads the additional weir input file. Various weir structures can be identified by different weir element types. Information for each weir element type is supposed to store in a set, which includes upstream, downstream water elevation and the corresponding discharge over the weir. These entries build a matrix relationship among them. The format of the input file will be shown in chapter 5.

Subroutine WTFORM

The information, which is read and stored by INCSTRC, is linearly interpolated in WTFORM. The weir overflow is interpolated according to upstream firstly and then downstream water elevation, which are passed from CSTRC2D for the previous iteration.

4.2.4. Time series

Subroutine INTIMES

This subroutine reads the time series file for hydraulic structures. The file can include the information for more than one hydraulic control structure, and each control structure is supposed to be able to be switched on and off many times.

Subroutine SWITON

The time read and stored in subroutine INTIMES is passed to SWITON, which compares this time with the actual time and decides whether the control structure is switched on or off. If the control structure is switched off, the discharge over the structure is set to be zero in CSTRC2D and jumped directly to the end of CSTRC2D.

4.3. Testing and adaptations

Extensive testing models have been built to examine the available functions in RMA-10S. The testing procedure is explained briefly in this chapter only in order to describe the adaptations made in the source code to solve the problems appeared in the testing models. Two models are depicted explicitly in the next chapter to verify the simulating function of hydraulic structures in RMA-10S and its necessary adaptations made during this master thesis. This chapter only concentrates on the modifications made in the source code.

4.3.1. General testing procedure

One part of the river Stoer is used to test the existing code for weir structure functions. It covers only the river bed from Willenscharen until the inflow of river Bramau. It is firstly simulated without any weir structure to obtain the initial starting solution. Then the weir structure is entered in the Kalypso-2D result file manually by re-identifying the element type. The weir overflow computation function is test afterwards.

It appears that if the newly inserted weir elevation is higher than water elevation, it would be very difficult to be converged. The scenario would be that water is suddenly cut off by the weir structure from the starting solution without weir. The downstream boundary condition has to be defined carefully under this circumstance in order to reach convergence. Therefore, it might be better to start the weir simulation from a high water elevation (higher than the weir crest). Water stage at the weir is supposed to decrease with decreasing input upstream discharge. However, it seems that after some time steps water is still flowing over the weir structure even if the water elevation is lower than the weir crest. Since the testing model used Kalypso-2D file as geometry input file and Microstation as the graphic interface tool, it is suspected that the cause would be the 2D geometry file or the connection of the interface between RMA-10S and the Kalypso-2D file. However, it also would be the problem with the existing code. The idea, to find out whether it is the problem with the 2D file, is to generate a binary geometry file based on this Kalypso-2D file and use this binary geometry file the same as the original geometry input file in RMA-10S.

The geometric information is written out in a file which maintains largely the format of the RM1 geometry file used in RMA-10S, but the head and continuity lines should be added manually in the RM1 file. This file can be either used directly in the simulation as geometry input or converted to binary geometry file (*.geo), and then use the binary file as geometry input. It was considerably difficult to be convergent to observe the influence of weir structure in this model, even if the converted geometry file is employed. In order to obtain the converged result, a much simpler channel is built for the testing purpose.

The simple trapezoidal channel is 50 meters wide and 2 km long with only 1 roughness class. For this channel it is much easier to get the converged simulation result. However, from the first simulation result, it seems that the weir structure does not work properly. Although the water elevation upstream is much higher than the weir elevation, water does not flow over the weir, but only along the weir segment.

After the first analysis, possible causes for the improperly functioned weir simulation would be:

- Since the element type for weir elements should be larger than 903, and this large number is normally not recognized in Microstation, the weir elements would not be recognized.
- According to the visualization result in RMAGEN, the direction of continuity lines is from right to left in the flow direction, which is opposite to Kalypso-2D. Therefore, the sequence of node numbering would also be the reason.

Further testing indicates that the first presumption can be simply excluded. It only causes problems when the roughness classes are visualized in Microstation. By using the converted geometry input file, it is already confirmed that the weir identifier is recognized in RMA-10S.

Testing for the second assumption suggests that the order of nodes for continuity lines is not important because the flow direction is defined again for each continuity line in the time step data block, and the simulation is based on the defined flow direction in this block. Although both assumptions have been excluded, attention to the different nodes sequence between the RMA-10S and Kalypso geometry input file has been raised. The source code of RMA-10S is analysed in the next step in order to detect the real reason.

After analysing the source code and testing with the models, it was affirmed that for weir elements there are special requirements of nodes numbering, so that the program can distinguish the upstream and downstream around the weir. The upstream side of the structure must be defined with sequence numbers 1, 2, and 3 (including mid-side node) of the element numbering sequence. The downstream side must be defined with sequence numbers 5, 6, and 7. The entire sequence must be numbered in an anti-clockwise sequence.

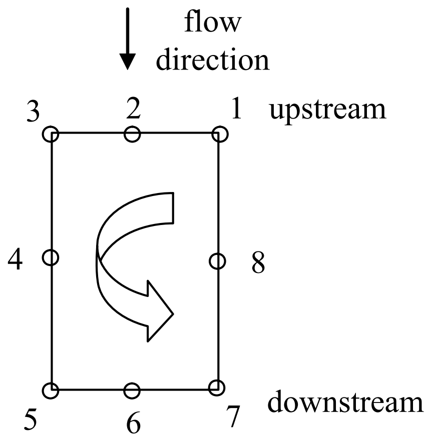

Figure 4.7 Nodes numbering sequence of a weir element

It is believed that the numbering sequence must be created when the mesh is generated in RMAGEN. It is also the sequence to define the nodes around a weir element. However, since Kalypso uses different graphic interface and geometry input file, the nodes numbering sequence is not automatically preserved in the Kalypso-2D geometry file. The nodes numbering sequence for weir elements like any other element in the Kalypso-2D file is counter clockwise, but the starting node is chosen randomly. Therefore, the defined upstream and downstream near the weir structure in subroutines CSTRC2D and WFORM are also randomly. The unreasonable simulation result is thus not surprising anymore.

In order to confirm that this was the real cause for the unreasonable simulation result, the node sequence of weir elements is firstly changed in the RM1 geometry file manually. This RM1 file is then used as the geometry input file for the weir simulation. The trial simulation appears to be valid. At least water flows over the weir crest at certain time steps. Thus, the next step is to implement automatic renumbering function in the source code for a better integration between the Kalypso-2D file and RMA-10S.

4.3.2. Adaptations

Renumber nodes' sequence for weir elements

Nodes' numbers are stored in a two-dimensional array NOP in the source code. The first index refers to the element number; while the second is for the number of nodes around the element. The sequence of nodes around an element is defined in the array. The initial concept to implement the automatic reordering of nodes for weir elements was to shift the nodes according to sequence defined at WDT lines in the control file. These shifted nodes are stored in another array which is used instead of NOP in subroutines related to weir structures. However, since NOP array is very commonly used in the whole program, it is indistinct when the reordered array should be used instead of NOP. Moreover, the NOP array can not be redefined in the weir subroutines, otherwise internal definition conflicts would occur.

After a short discussion, it is suggested that the NOP array should be redefined for weir elements when it is initialized in subroutine RDKALYPSO. RDKALYPSO is the core subroutine to read the geometry input file in the Kalypso-2D format. The idea is to add the starting node for weir elements at the end of FE lines in the Kalypso-2D file. This information is read in RDKALYPS subroutine and stored in the two-dimensional array REWEIR, which records the weir element number and its starting node. After reading and establishing all the element information, subroutine REWEIR2DKALYPSO is called if there are weir elements in the mesh, and their first nodes defined in NOP are not the same as the input starting nodes. This subroutine reorders the nodes' sequence around an element according to the recorded starting node. The starting node for a weir element is also written out at the end of the FE lines in the result 2D file, so that the restart by using the result 2D file is enabled without entering the starting nodes again at FE lines.

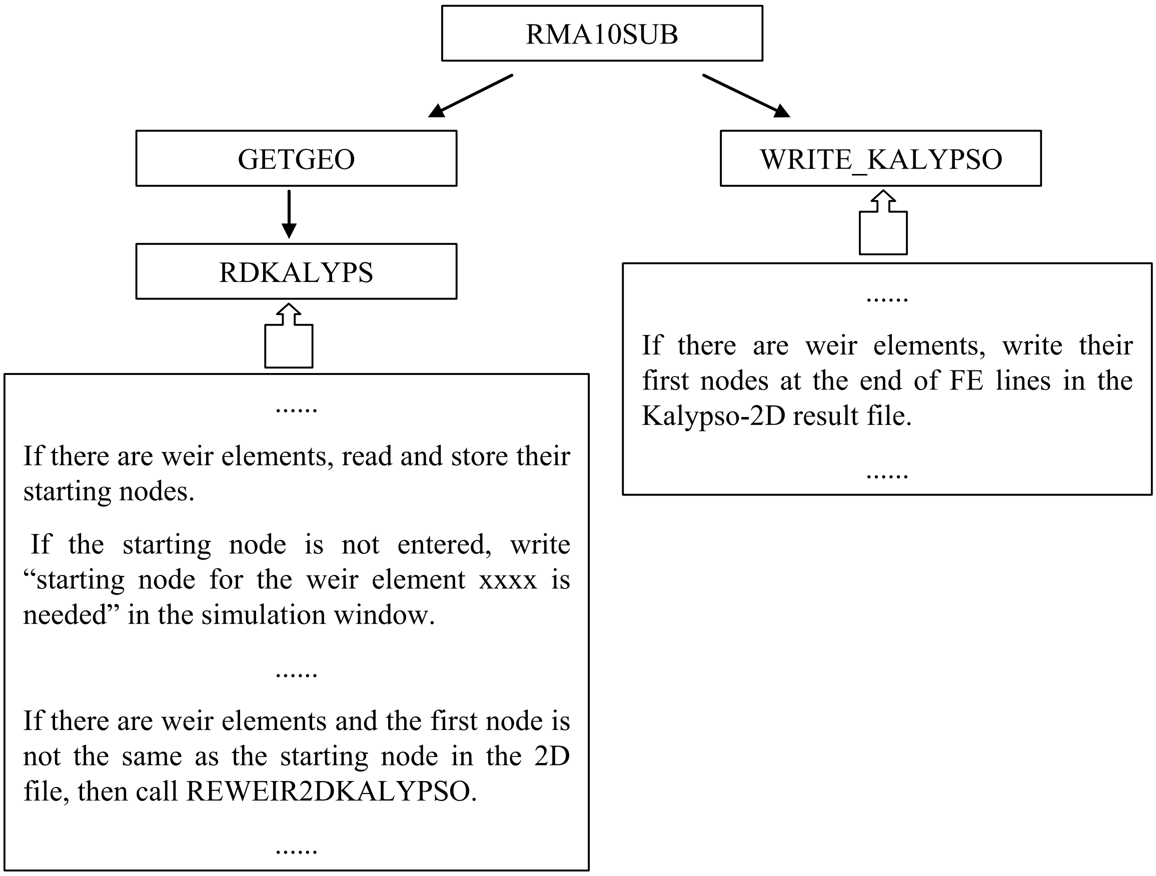

Figure 4.8 Flowchart for renumbering nodes sequence of weir elements

Read the weir overflow input file

The function of reading and linear interpolating the weir overflow input file has also been tested. It worked properly with one weir data set. However, when there is more than one weir element type, which means more than one weir data set has to be entered, it stopped automatically after reading the first data set. Some changes have been made in subroutine INCSTRC accordingly. After debugging, it is now able to read the input discharge matrix and interpolate the discharge over weir.

Time series to switch the control structure on and off

Subroutine INTIMES is tested for its function to read the time series input file. It is supposed to be capable to read many entries of switch on and off time series for more than one control structures. However, the testing shows that when there is more than one time series entry (NTV lines) for any of the weir, it stopped after reading the first NTV line of that control structure. Debugging is thus required to read the time information for more than one control structure and more than one NTV entry for each control structure.

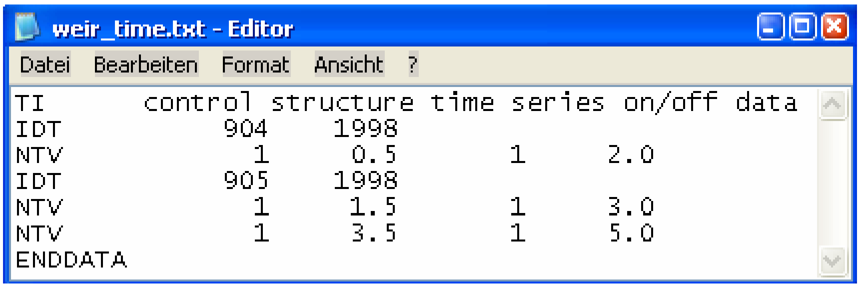


```
TI      control structure time series on/off data
IDT          904     1998
NTV            1      0.5        1      2.0
IDT          905     1998
NTV            1      1.5        1      3.0
NTV            1      3.5        1      5.0
ENDDATA
```

Figure 4.9 An example of time series input file for control structures

An example of the time series text input file is demonstrated above. A short explanation of each identification line is as follows:

TI: title for the file

IDT: control structure definition data line. Element type number for the control structure and the year for data set should be entered in this line.

NTV: line for control structure on / off times, can be repeated as many lines as required. The date and hour to switch the structure on and off should be entered in this line sequentially.

Each entry of this file occupies 8 spaces and each numerical entry is left adjusted. IDT and NTV lines can be repeated for each control structure element type that is to be defined. (King, 2005a)

5. Verification

Two models are illustrated in this chapter to analyse the validity of this function: one is the simple trapezoidal channel and the other is one part of the river bed in the river Stoer. Only the simulated result with one weir structure is demonstrated in this chapter for verification. However, it was also tested that the program was able to simulate with more than one weir structures at different locations or one weir structure but with different properties for weir segments. It is enabled by identifying the weir elements with different element type numbers.

In order to verify the control structure simulation result, simulation information around the weir is written out in text files. This function is only for the internal check in the scope of this master thesis, and is not yet ideally implemented in the source code. It is shortly explained below, and the results of both testing models are obtained directly from this function.

The discharge over the whole weir is calculated and output in the text file QWEIR.TXT for each iteration. The discharge is calculated in the subroutine CSTRC2D primarily for the whole weir element using the unit width discharge (averaged by the two corner nodes) multiplying the element width. The calculated element discharge is then summed up for each weir structure with the same element type. This function is also available when there is more than one weir structure. However, the discharge is only calculated in CSTRC2D. Thus if the weir element is submerged and CSTRC2D is not called any more, discharge over this weir element is then not calculated and regarded as zero. In this case, the result in QWEIR.TXT is misleading. Therefore, only the discharge, when the weir structure is not submerged, is considered for verification. Furthermore, since the discharge calculated in CSTRC2D, WFORM or WTFORM is based on the water elevation from previous iteration, the discharge in QWEIR.TXT should be shifted one iteration prior in order to validate the actual result.

Further information (upstream and downstream water elevation and upstream velocity) around the weir is leveraged along the whole weir structure and recorded in the text file HWEIR.TXT for each iteration. It works properly only when there is one weir element type. This information is used to validate the weir overflow in QWEIR.TXT. These two text files have to be deleted each time before starting the new simulation.

5.1. Testing channel

5.1.1. Channel profile

The small testing channel is generated by the program "make_channel_0_2_1.exe" only for the quick check purpose. It is 50 meters wide, 2000 meters long. There are 2 elements for the main channel (each element is 20 meters wide), and two bank elements at each side (5 meters wide each, and with the bottom elevation 2 meters from the main channel). In order to avoid any negative bottom elevation, the elevation at each node has been enhanced by 100 meters. This means that the bottom elevation at the upstream in the main channel is 100 meters above sea level and 102 meters above sea level at the banks. There are 50 elements in total in the longitudinal direction, with 40 meters long each. The slope of the channel is 0.001. Only one roughness class is specified in the model to simplify the simulation. The profile is illustrated in the following figure.

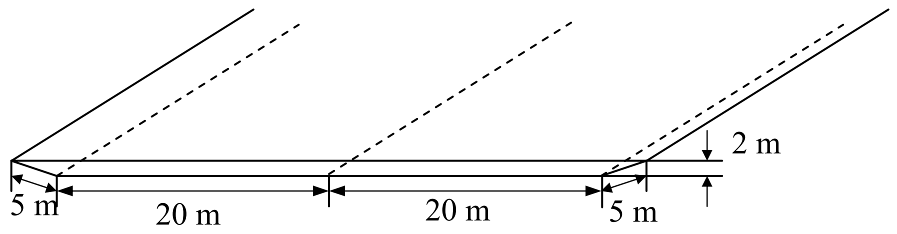

Figure 5.1 Profile of the testing channel

5.1.2. Simulation input

The weir structure is placed in the middle from upstream and downstream across the whole channel. The weir crest is set to be 108 meters which is 9 meters higher than the bottom elevation in the river bed. It is set relatively high in order to observe the weir overflow procedure. The transition elevation, at which the Navier-Stokes-Equation should be used for weir elements instead of the weir equation, is specified as 109 meters. The length of the weir highroad in the flow direction is 5 meters. These weir data are defined in the control file at WDT lines for each node at upstream or/and downstream of weir elements. Additional roughness class for weir elements is also specified in the control file. Identification line FC is added in the time step block for the weir structure continuity line. All the information is entered in the control file which is shown below, followed by a short explanation of the weir relevant data blocks.

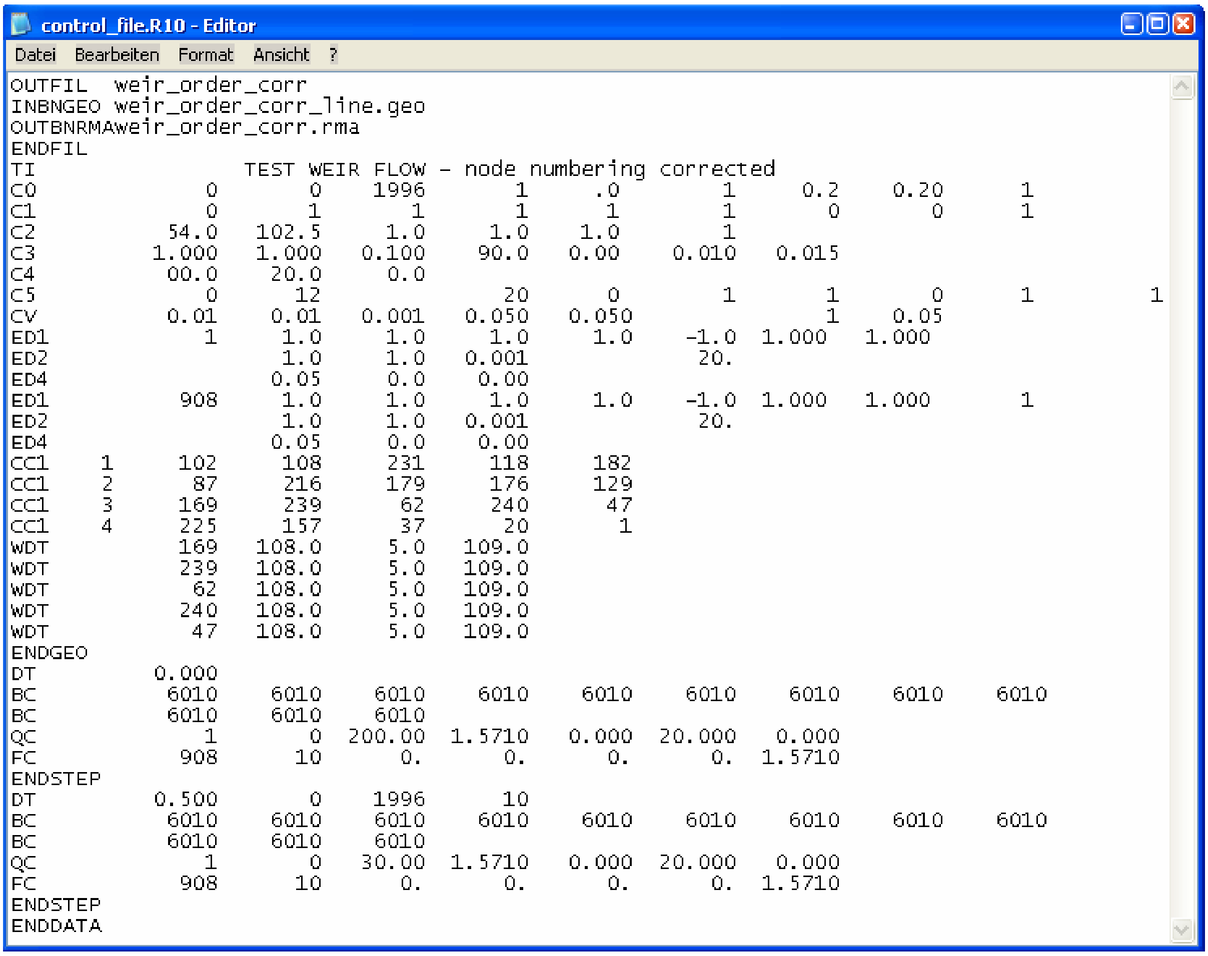

control_file.R10 - Editor

Datei Bearbeiten Format Ansicht ?

```
OUTFIL   weir_order_corr
INBNGEO weir_order_corr_line.geo
OUTBNRMAweir_order_corr.rma
ENDFIL
TI                 TEST WEIR FLOW - node numbering corrected
C0             0       0    1996       1      .0       1     0.2    0.20       1
C1             0       1       1       1       1       1       0       0       1
C2          54.0   102.5     1.0     1.0     1.0       1
C3         1.000   1.000   0.100    90.0    0.00   0.010   0.015
C4          00.0    20.0     0.0
C5             0      12              20       0       1       1       0       1         1
CV          0.01    0.01   0.001   0.050   0.050               1    0.05
ED1            1     1.0     1.0     1.0     1.0    -1.0   1.000   1.000
ED2                  1.0     1.0   0.001             20.
ED4                 0.05     0.0    0.00
ED1          908     1.0     1.0     1.0     1.0    -1.0   1.000   1.000       1
ED2                  1.0     1.0   0.001             20.
ED4                 0.05     0.0    0.00
CC1     1    102     108     231     118     182
CC1     2     87     216     179     176     129
CC1     3    169     239      62     240      47
CC1     4    225     157      37      20       1
WDT          169   108.0     5.0   109.0
WDT          239   108.0     5.0   109.0
WDT           62   108.0     5.0   109.0
WDT          240   108.0     5.0   109.0
WDT           47   108.0     5.0   109.0
ENDGEO
DT         0.000
BC          6010    6010    6010    6010    6010    6010    6010    6010    6010
BC          6010    6010    6010
QC             1       0  200.00  1.5710   0.000  20.000   0.000
FC           908      10      0.      0.      0.      0.  1.5710
ENDSTEP
DT         0.500       0    1996      10
BC          6010    6010    6010    6010    6010    6010    6010    6010    6010
BC          6010    6010    6010
QC             1       0   30.00  1.5710   0.000  20.000   0.000
FC           908      10      0.      0.      0.      0.  1.5710
ENDSTEP
ENDDATA
```

Figure 5.2 Control file for the testing channel

WDT lines are specified after the continuity lines are defined in the properties data block. They are only needed if the control structure type 10 is used on the FC data line and the weir overflow input file is not used. In this line, node number (supposed to be on the notional upstream side), elevation of weir crest, length of weir crest in the flow direction, and transition elevation should be entered sequentially. On the FC line, weir element type and the type of control structure are defined at first. If the control structure is a weir (type 10 in this case), the following 4 parameters are not in use. Only the last entry, which indicates the flow direction over the weir, is used. It is calculated in the unit of radian starting from the x axis counter-clockwise. Each entry mentioned above occupies 8 spaces and is right adjusted as most cases for the input file if not specified.

The discharge 30 m^3/s from upstream is defined as the upstream boundary condition. This is the suitable discharge, with which we can observe the weir overflow distinctly. No downstream boundary condition is specified, because it appears that it is much easier to converge without any downstream boundary condition for the testing channel. The same input boundary is simulated for 20 time steps, half an hour for each time step interval.

5.1.3. Simulation result

In order to validate the result calculated in RMA-10S, the output weir overflow from the program is compared to the overflow calculated by POLENI formula.

$$Q = \frac{2}{3}\mu b\sqrt{2gh^3}$$

where 0.5 is taken as the value for μ, 50 for the weir width normal to the flow direction and h is the upstream water depth over the weir. The submergence coefficient is computed as:

$$C_{sub} = \sqrt{1 - \left(\frac{t}{h}\right)^n}$$

where $n = 16$, t and h are the water depths over the weir upstream and downstream at the weir structure.

Results are illustrated as follows and only compared until when the weir is submerged.

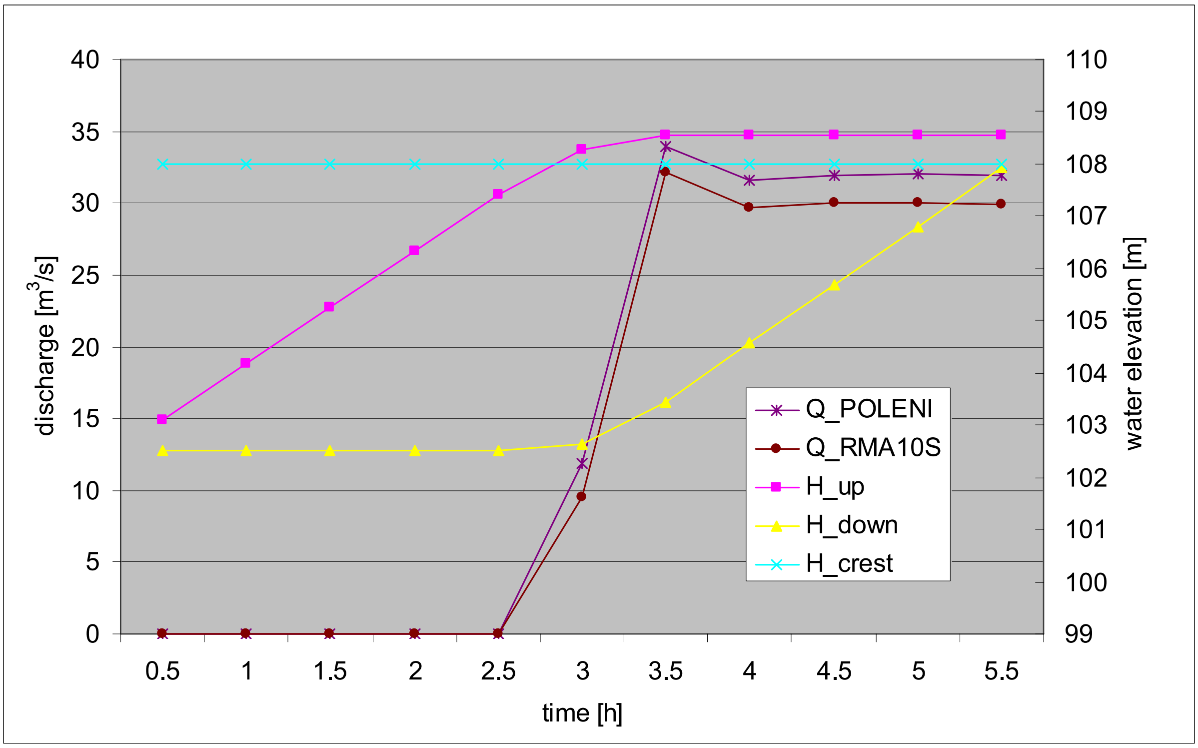

Figure 5.3 Results verification of the testing channel

The result appears to be plausible that water starts to flow over the weir at the right time (after 2.5 hours), when the water elevation at upstream around the weir starts to be higher than the weir crest. The largest difference between the simulated weir overflow by RMA-10S and the manually calculated one (based on POLENI formula) is about 2 m^3/s. There are several arguments to explain the difference:

- The model simulated in RMA-10S has 30 m^3/s discharge as the upstream boundary condition. The computation of weir overflow in this case should not only consider the weir equation but also the continuity equation. Therefore, when the weir overflow becomes more stable, it tends to be restricted to 30 m^3/s instead of 32 m^3/s which is calculated only with POLENI equation.
- The discharge, computed by RMA-10S and written out in QWEIR.TXT, is firstly calculated for each weir element and then summed up for the whole weir structure. While the weir overflow calculated with POLENI equation is calculated by using the average upstream water depth over the weir multiplying the weir length. It is therefore also likely to have any difference due to numerical reasons.
- Since the two theories differ significantly from each other, it is also not surprising to have slight difference between the two discharges derived from these theories.

The downstream water elevation around the weir is rising continuously after water starts flowing over. The reason would mainly be that there is no downstream boundary condition specified in the control file; hence the program may assume that no water flows out of the channel. It is a very practical method to observe the backwater effect with the rising downstream water elevation. After 5.5 hours, the water elevation at the downstream side of the weir exceeds the defined weir crest elevation; then the weir elements are set to be submerged and the weir overflow is not calculated by the weir equation.

From the first validation result, it would be concluded that the function of simulating control structures like weirs worked properly after the adaptation of the Kalypso-2D file into RMA-10S. Small difference between the simulation result and the POLENI formula is observed. However, it is still in the acceptable range.

5.2. Implementation for the river Stoer

The tested program is implemented in the Stoer model, with which both weir computation function and the weir overflow input function are carried out. The results are then compared for a further verification.

5.2.1. Model description

The Stoer is a river in Schleswig-Holstein, Germany, a tributary of the Elbe. It originates east of the Neumünster, and flows west through Neumünster, Kellinghusen, and Itzehoe, with a total length of 87 km. The Stoer joins the Elbe near Glückstadt. Tide influences the water stand in the Stoer more than half of its length, up to the gauging station Rensing about 1 km away from Kellinghusen. Shortly before the estuary, there is a closing structure to protect the Stoer from the extreme effect of storm tides.

In order to designate flooding areas along the river and determine the damage risk map, regeneration of the Stoer became one of the research and development projects at the Institute of River and Coastal Engineering, Hamburg University of Technology. Several two-dimensional flow models have already developed for this project. The testing model took the mesh of river bed from Willenscharen until the inflow of the river Bramau.

There are two bridges in the original model. Some elements for these bridges are deactivated in the original mesh. The weir structure is built near the bridge at downstream across the whole main channel. The original downstream bridge elements are activated. Elements aside the weir are deactivated, so that water can only flow over the weir. The other bridge upstream remains the same.

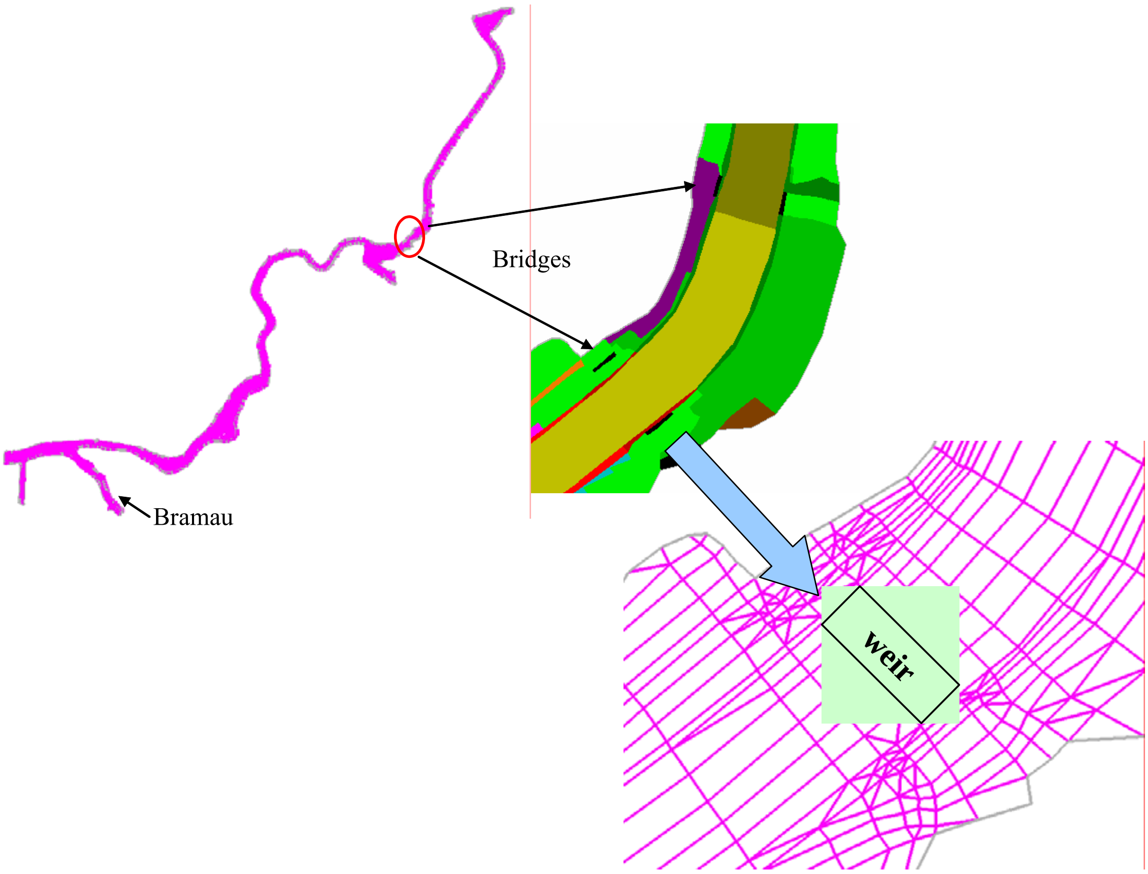

Figure 5.4 Mesh of the testing model: the Stoer

5.2.2. Model input

The model is simulated both with and without weir overflow input file. Including weir elements there are 20 roughness classes specified in the model. Two discharge inflow boundary conditions are from upstream and the Bramau. Downstream water elevation is also defined in the control file. The bottom elevation in the main channel is about 0 m above the sea level, and the width is about 20 meters. The model is able to simulate the weir overflow with various weir crest elevation. However, since it would be more convenient to calculate the weir overflow per unit width for the input file, the weir crest is set to 6.5 meters cross the whole river in order to observe the weir overflow process. The transition elevation is set to 7 meters and the weir width in the flow direction is 5 meters.

The model is simulated with steady flow without the weir structure at first. Large discharges 35 m^3/s and 14.7 m^3/s are defined for the upstream and Bramau inflow respectively. Downstream water elevation is fixed to 2.3 meters. The steady result is utilized as the starting solution for the unsteady simulation with the weir.

To start simulating with the weir, roughness classes for weir elements should be changed to the correct number (from 904 to 989), and the starting node for each weir element should be entered at the end of FE line in the Kalypso-2D file. One flood wave is simulated starting from high water stand. 22 time steps are simulated with 1 hour time interval each. The input boundary conditions are shown in the following figure.

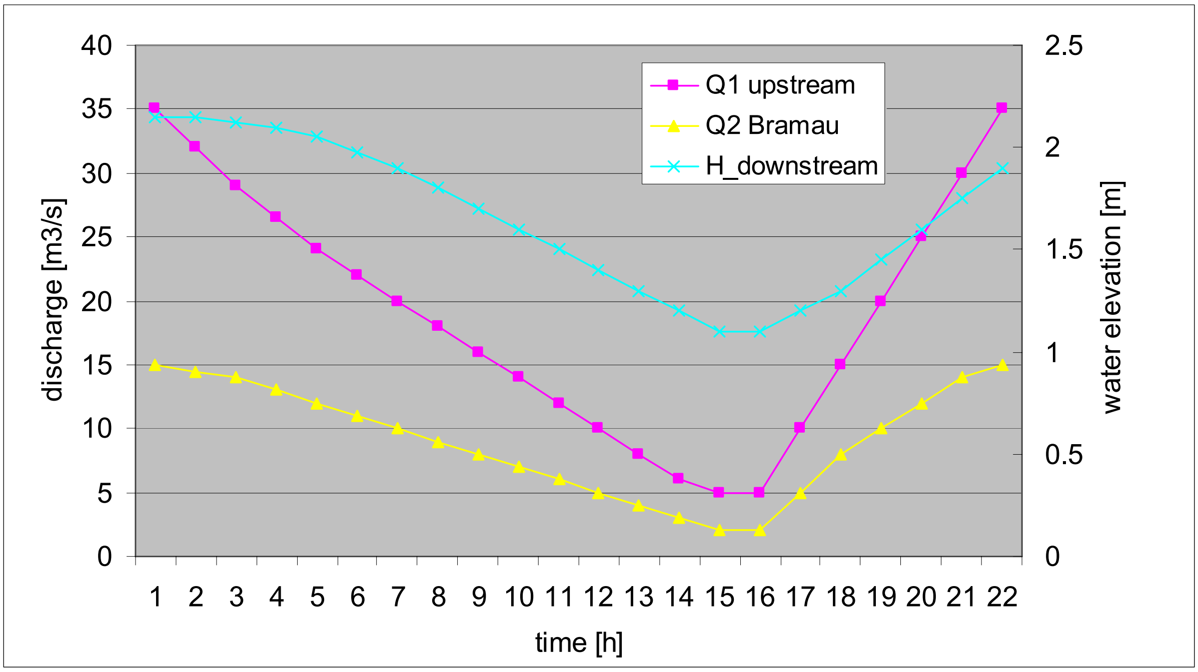

Figure 5.5 Input boundary conditions for the Stoer model

The same input condition is also used for the simulation with weir overflow input file. The overflow is calculated with POLENI formula per unit width. It is supposed that when the weir input file is used, the horizontal weir crest has to be assumed for each defined weir element type, since the same data will be shared for all elements defined with this element type. Therefore, if various weir crest elevation has to be implemented, different weir element types would have to be defined for each weir segment.

This file has to be created manually. The weir overflow discharge can be obtained from other hydraulic models or calculated as in the Stoer model. The value of the upstream and downstream water elevation entered in the text file should be selected carefully. If no reference value is found in the file, the weir overflow would be set to zero. The format and calculation result are shown below. Meaning of each identification line is explained afterwards.

weir.txt - Editor

Datei Bearbeiten Format Ansicht ?

```
TI      weir testing 2
IDC         904      14       7
HRW         0.0     3.0     4.0     5.0     6.0     7.0     8.0     9.0    10.0
HRW        11.0    12.0    13.0    14.0    15.0
HCL         0.0     1.0     1.5     2.0     2.5     3.0     3.5
FLW         0.0     0.0     0.0     0.0     0.0     0.0     0.0
FLW         0.0     0.0     0.0     0.0     0.0     0.0     0.0
FLW         0.0     0.0     0.0     0.0     0.0     0.0     0.0
FLW         0.0     0.0     0.0     0.0     0.0     0.0     0.0
FLW         0.0     0.0     0.0     0.0     0.0     0.0     0.0
FLW        0.52    0.52    0.52    0.52    0.52    0.52    0.52
FLW        2.71    2.71    2.71    2.71    2.71    2.71    2.71
FLW        5.83    5.83    5.83    5.83    5.83    5.83    5.83
FLW        9.66    9.66    9.66    9.66    9.66    9.66    9.66
FLW       14.10   14.10   14.10   14.10   14.10   14.10   14.10
FLW       19.04   19.04   19.04   19.04   19.04   19.04   19.04
FLW       24.46   24.46   24.46   24.46   24.46   24.46   24.46
FLW       30.32   30.32   30.32   30.32   30.32   30.32   30.32
FLW       36.58   36.58   36.58   36.58   36.58   36.58   36.58
ENDDATA
```

Figure 5.6 Weir over flow input file

TI: title for the file.

IDC: control structure definition data. In this line, element type, number of rows and columns for this element type should be defined sequentially.

HRW: upstream water surface elevations, maximum 9 entries per line, as many lines as required.

HCL: downstream water surface elevations, maximum 9 entries per line, as many lines as required.

FLW: flow for the corresponding row and column elevation defined earlier. Enter row wise (the whole line corresponds to the same upstream water surface elevation). One entry in the line is for the related column. Repeat as many lines as entries of upstream water surface elevations. Note that the values are in m^3/s per unit width, maximum 9 entries per line.

IDC, HRW, HCL and FLW should be repeated as many as weir element types defined in the model.

5.2.3. Simulation result

The simulation results with both methods are shown in Figure 5.7.

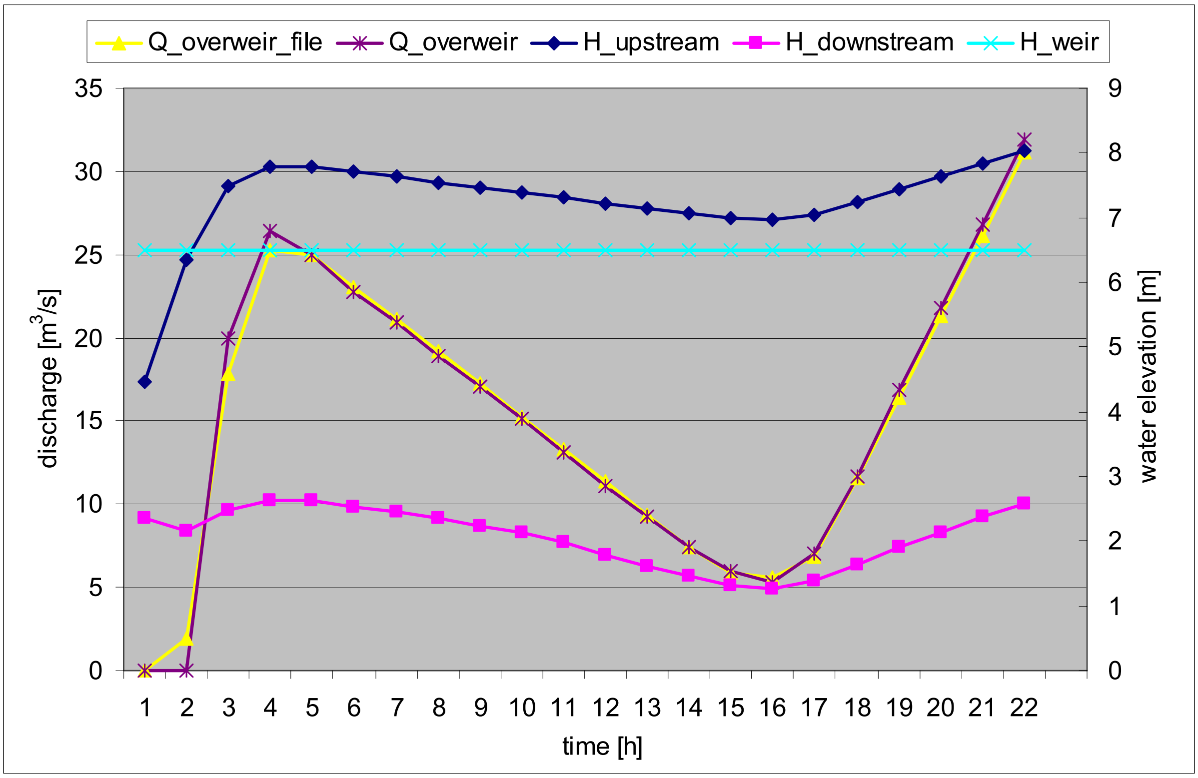

Figure 5.7 Simulation results of the Stoer model

This figure shows a very satisfactory result. The largest difference occurs when water starts to flow over the weir until it reaches the peak of the overflow amount. At the second time step, the water surface elevation at the upstream weir is about 6.3 m which is lower than the weir crest 6.5 m. However, since the weir overflow input file only gives the value with the weir upstream water elevation 6 and 7 meter, weir overflow is already interpolated at 6.3 m from the input values. Larger difference takes place when large change of weir overflow occurs. Nevertheless, it is still in the range of 1 to 2 m^3/s. At other time steps it has an agreeable match with the computed result from RMA-10S.

The downstream water surface elevation near the weir stays always significantly lower than the weir crest. Therefore, no real backwater effect can be studied. This is mainly due to the defined low downstream water elevation at the outflow boundary. Downstream boundary conditions should be defined carefully in order to obtain convergence. In some cases, the influence of the possible weir overflow should also be considered.

Since the simulated results from two approaches do not differ considerably, in most cases the weir structures in hydraulic models can be simulated by any approach. The selection of the simulation method (whether the weir overflow should be computed by the program or entered externally) depends on the situation in each model, and each method has its own advantages.

If the weir crest is not horizontal and various crest elevation is expected, it would be much more convenient to use the implemented formula in the source code to calculate the weir overflow. In this case, the individual weir crest elevation can be entered at WDT lines in the control file. If the weir input file is used to interpolate the weir overflow, many weir element types would have to be defined for weir segments with different weir crest elevation, and the overflow values would have to be entered for each weir element type.

Suppose that the whole weir structure has the same crest elevation, and the discharge of the weir overflow is already available from other hydraulic models or derived from other formulas, then the external weir input file would be more advantageous. It saves the calculation time and is more flexible regarding to the implemented formulas. However, the upstream and downstream water levels should be chosen carefully in order to acquire more accurate result. For example, in the Stoer model one more value 6.5 should be added for upstream water level, since the weir crest is set to 6.5 meters. Selecting and testing the correct values and creating the file manually sometimes also take considerable amount of time.

With regard to the convergence and accuracy, these two approaches do not differ evidently from each other in the testing models. It appears, nevertheless, that by using the external weir input file it would be easier to converge.

6. Conclusion and further remarks

Since the function of modelling hydraulic structures by two-dimensional flow models is already available in RMA-10S, the primarily defined objective of this master thesis has been adjusted to understand and test the existing function in the program. If necessary, modifications also have to be made in the source code. Although the original RMA-10S program has been extended to be capable to read and write the Kalypso-2D geometry files, potential integration problem may still exists. After extensive tests, it is confirmed that the problem causing incorrect simulation results is due to the nodes' sequence around weir elements defined in the geometry file. Adjustment has been made to reorder the nodes for weir elements in Kalypso-2d models. Other modifications related to the hydraulic structures simulation have also been accomplished in the source code. The existing functions together with the modifications in RMA-10S have been tested and verified by several models. The simulation results are compared with the results calculated by POLENI formula, which was originally defined for the weir simulation. The comparison demonstrates that the difference between the weir equation implemented in RMA-10S and POLENI formula is marginal. Furthermore, the weir overflow calculated by other formulas can always be entered in weir input file, which will be interpolated by the model. Therefore, further implementation of other weir formulas is not absolutely necessary.

Within this master thesis, the weir simulation results are only tested with the implemented weir equations. When weir elements are submerged and regarded as normal elements, the structure has to be simulated by giving a special roughness class. What is the requirement of the roughness parameters and how effective it is to consider the hydraulic structure are not analysed in the work. The criteria to select the transition elevation, at which the weir structure can be considered by bottom roughness, are not clearly stated, either. Further discussion is required to define these parameters.

The implementation of hydraulic structures as one-dimensional elements would also be possible in the existing RMA-10S. Subroutine CSTRC, which has the similar function as CSTRC2D for two-dimensional elements, is already available in the source code. The principle of simulating hydraulic structures with one-dimensional models would also be deducted on the basis of this master thesis.

One remark, which still has to be mentioned regarding to the existing program, is the determination of when the weir equation should be used. Currently it is set that as long as the weir element is submerged, Navier-Stokes equations are then used instead of the weir equation. However, apparently it would be more reasonable to determine it just according to the input the transition elevation.

7. References

Cigana, J., Basement floodings: relieving the hydraulic grade line (HGL) with proportional overflow devices, John Meunier Products / US Filter, Canada

Franz, D. D. and Melching, C. S. (2004) Full Equations Utilities (FEQUTL) Model for the Approximation of Hydraulic Characteristics of Open Channels and Control Structures During Unsteady Flow, Water Resources Investigations Report 97-4037, U.S. Geological Survey, online, available at: http://il.water.usgs.gov/proj/feq/fequtl/fequtl.toc_1.html

Hulsing, H. (1967) Measurement of peak discharge at dams by indirect methods: Techniques of Water-Resources Investigations of the United States Geological Survey, Book 3, Chapter A5

Hutton, D. (2004) Fundamentals of Finite Element Analysis, McGraw-Hill Higher Education, New York, America

Institute of River and Coastal Engineering (2005), 1D Hydraulic Simulation, chapter 6, Hamburg University of Technology, Germany

Institute of River and Coastal Engineering (2006), Lecture Notes: Environmental Hydraulic Simulation, Hamburg University of Technology, Germany

Kindsvater, C.E. (1964) Discharge characteristics of embankment-shaped weirs: U.S. Geological Survey Water-Supply Paper 1617-A, Studies of flow of water over weirs and dams, Prepared in cooperation with the Georgia Institute of Technology

King, I. P. (1993) RMA-10 A Finite Element Model for Three-Dimensional Density Stratified Flow, Department of Civil and Environmental Engineering, University of California Davis

King, I. P. (2005a) A Finite Element Model for Stratified Flow and Cohesive Sediment/Sand Transport RMA-10S, User Guide Version 3.4, Sydney, NSW Australia

Pasche, E., Monitoring and Assessment in Rivers Based on Two-Dimensional Models, Chief Division Hydroinformatics, Björnsen Consulting Engineers, Koblenz, Germany

Peter, G., The discharge and run off calculation of weirs under the consideration of dynamic flows, Fachhochschule Magdeburg, Fachbereich Wasserwirtschaft, Germany

Ploeger, W. (2004) Kalypso 2D Documentation, version 1.2, Institute of River and Coastal Engineering, Hamburg University of Technology, Germany

Reddy, J. N. (1993) An Introduction to the Finite Element Method (2^{nd} ed.), McGraw-Hill, the United States of America

Schrage, N. (2006) Abschlussarbeit: Entwicklung eines Gekoppelten 1D-2D-Strömungsmodells zur Optimierung der Bestimmung von Überschwemmungsgebieten, Institute of River and Coastal Engineering, Hamburg University of Technology, Germany

Zienkiewicz, O. C. and Taylor, R. L. (2000) The Finite Element Method: Volume 3 Fluid Dynamics (5^{th} Edition), Butterworth-Heinemann, Oxford, Great Britain

Bibliography

Baresel, C. (2001) Diplom Thesis: 1D – Channel Flow, Implementation of the St. Venant Equations into the One-Dimensional Finite Element Method, Institute of River and Coastal Engineering, Hamburg University of Technology, Germany

Bund der Ingenieure für Wasserwirtschaft, Abfallwirtschaft und Kulturbau [BWK] e.V. (1999) Hydraulische Berechnung von Naturnahen Fließgewässern, Teil 1, Stationäre Berechnung der Wasserspiegellinie unter besonderer Berücksichtigung von Bewuchs- und Bauwerkseinfüssen, Düsseldorf, Germany

Carey, G. F. and Oden, J. T. (1986) Finite Elements: Fluid Mechanics (Volume VI), Prentice-Hall, the United States of America

Chandrupatla, T. R, and Belegundu, A. D. (2002) Introduction to Finite Elements in Engineering (3rd Edition), Pearson Education International, USA

Chapman, S. J. (2004) Fortran 90/95 for Scientists and Engineers (2nd Edition), McGraw-Hill, Singapore

Chow, V. T. (1973) Open-Channel Hydraulics, McGraw-Hill, Inc., Singapore

Horton, R.E. (1907) Weir experiments, coefficients, and formulas: U.S. Geological Survey Water Supply and Irrigation Paper 200, Series M, General Hydrographic Investigations, 24, Revision of Paper No. 150, Department of the Interior United States Geological Survey

King, I. P. (2005b) RMAGEN: A Program for Generation of Finite Element Networks, User Instructions, Version 7.3e, Sydney, Australia

King, I. P. (2005c) RMAPLT: A Program for Displaying Results from RMA Finite Element Programs, User Instructions, Version 7.3e, Sydney, Australia

King, I. P. (2005d) Update Documentation: RMA2 – A Two Dimensional Finite Element Model for Flow in Estuaries and Streams, Version 7.4G, Sydney, Australia

Lahey/Fujitsu Fortran 95, Language Reference, Revision D, Lahey Computer Systems, Inc.

Teschke, U. and Töppel, M. (2004) Lösung einer gwöhnlichen DGL mit FEM and FDM, Version 1.1, vom 14. Januar 2004, Institute of River and Coastal Engineering, Hamburg University of Technology, Germany

Appendixes

Appendix I – Variable list related to hydraulic structure simulation

Symbols	Index	Description
ALFA	np	array of boundary slopes
ALTMP		tangent value from node 1 to 7, 2 to 6, or 3 to 5 in one element
AO	np	array of bed elevation
CORD	np,3	array of nodal cordinates
CTIMEOF	ntimset,ntimemx	time for switch off the weir structure, converted to hours in year (NTIMSET: number of time data sets for each weir element type, NTIMEMX: number of entries for on/off sequence)
CTIMEON	ntimset,ntimemx	time for switch on the weir structure, converted to hours in year (NTIMSET: number of time data sets for each weir element type, NTIMEMX: number of entries for on/off sequence)
DH		downstream level above bed
DOH		ratio of downstream depth over weir to upstream head. DOH=DH/HEAD
DV		downstream velocity
DW		downstream water surface level
EC		elevation of weir crest
FLW	nsets,nrowm,ncolm	flow for each set of weir data and for each row and column elevation defined by the above two variables
HCL	nsets,nrowm	upstream water surface elevation (NSETS is the number of weir data sets or the number of weir types; NROWM is the maximal number of HRW entries in this file)
HEAD		upstream energy head
HEAD2		downstream energy head
HOL		ratio of head to length of crest
HRW	nsets,nrowm	downstream water surface level (NSETS is the number of weir data sets or the number of weir types; NROWM is the maximal number of HRW entries in this file)
IMAT	NE	array of element characteristics number
ISUBM	nop(nn,L)	whether the node is submerged (nn: element number, L: the number of the node within this element, nop: node number). 0: not submerged, water level lower than the weir elevation; 1: submerged, higher than weir elevation or transition elevation; 2: the same node not submerged at previous iteration, but submerged at this iteration, boundary node, not in consideration; -1: initialized
ISUBMEL	(nn)	whether the element is submerged (nn: element number). 1: is submerged; 0: not submerged, then CSTRC is called for the weir structure

Symbols	Index	Description
ITP		switch controlling surface type. 0: paved; 1: gravel.
ITYP		0: discharge over the weir is 0; 1: not submerged; 2: submerged, get submergence correction; 3: totally submerged.
L		width of crest normal to the flow direction
MAXA		number of arcs
MAXN		actual iteration number, first initialized, then incremented
MAXT		number of transition elements
NCORN	NE	array of number of nodes around an element
NDEP	NPM	array of number of nodes in vertical line below
NE		number of elements
NEM		number of surface elements
NETYP	NE	array of defining element type
NFIX	NP	array of boundary conditions
NFIX1	NP	continuation array of BC's
NFIXH	NE	array containing element elimination order
NITA		maximum number of iterations of timestep, local copy
NITN		maximum number of iterations of timestep, global value
NOP	NE,20	array of nodes forming an element
NP		number of nodes
NPM		number of surface nodes
NREF	NPM	array showing nodes below a fvien surface node
NSURF	NP	array of surface node number above this node
NTMREF	IMAT(NN)	indicates the time set data for control structure. Initial value is 0. if there is a separate file for the control structure time series of on/off data, it equals the current number of data set (IDT lines). If there is no such time file, it remains 0.
NTR		actual iteration number, 0: steady start; 1: dynamic start; >1: during iteration
Q		flow per unit width
SE		ratio of heads upstreams to downstream. SE=HEAD2/HEAD
SPEC	np,3	array of specified BC's
SWITOF		variable to indicate whether the weir structure is switched on or off (1: off, 0: on)
TH	NE	array of principal direction of element
TRANSEL	nop(nn,L)	transition water elevation between free and submerged flow. (nn: element number, L: the number of node within this element, nop: node number), entered at WDT line in the control file
U	N	flow velocity at the Nth node in the weir element in the direction of the arc and the flow direction
UH		upstream level above bed
UV		upstream velocity
V	N	flow velocity at the Nth node in the weir element in the direction of the arc and perpendicular to the flow direction

Symbols	Index	Description
W		upstream water surface elevation
WHGT	nop(nn,L)	weir crest elevation, the format is the same as TRANSEL entered at WDT line in the control file
WIDEM		total embankment width. E.g. the distance from node 1 to 7, 3 to 5 and 2 to 6 around one element
WIDTH	NP	array of bed widths for 1D nodes
WSLL	nop(nn,L)	calculated water elevation, especially for weir structure

Appendix II – User guide for 2D hydraulic structure simulation

This user guide is targeted to give future users a quick introduction how to build and simulate a model with hydraulic structures and what related major functions are available in the current RMA-10S version. It is able to calculate weir overflow with varied weir crest for several defined weir structures. This function can be replaced by a weir overflow input file with which the input weir overflow can be read and interpolated.

The first step is to identify the location of the hydraulic structures (e.g. weirs) and elements which should be defined as weir elements (with element type between 904 and 989). If Kalypso-2D file is used as the geometry input file, the element type of weir elements should be changed at FE lines in the Kalypso-2D file. Furthermore, the starting node for the weir element should be entered at the end of the line (definition of the starting node please refer to chapter 4.3.1 of the master thesis).

Line	Example of FE lines in the Kalypso-2D file					
1	FE	1204	43	43	2932	
2	FE	1205	908	908	2931	2231
3	FE	1206	43	43	1257	

In the figure above line 2 is an example of defining weir elements in the FE line. The additional information is the starting node around element 1205. The starting node is defined as node 1 in the following figure for each element.

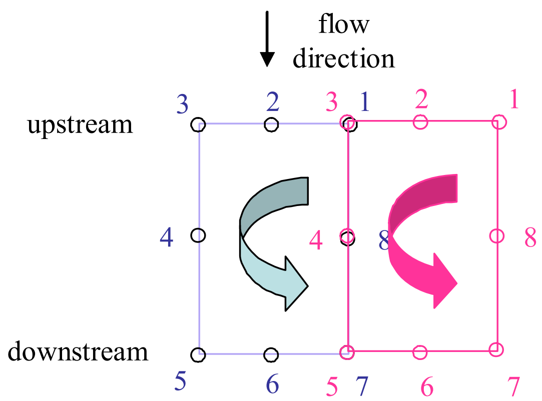

Afterwards some weir information should be entered in the control file to facilitate the simulation. One example, which has been shown in 5.1.2, is illustrated as follows.

control_file.R10 - Editor

Datei Bearbeiten Format Ansicht ?

```
OUTFIL   weir_order_corr
INBNGEO weir_order_corr_line.geo
OUTBNRMAweir_order_corr.rma
ENDFIL
TI                TEST WEIR FLOW - node numbering corrected
C0            0       0    1996       1      .0       1     0.2    0.20       1
C1            0       1       1       1       1       1       0       0       1
C2         54.0   102.5     1.0     1.0     1.0       1
C3        1.000   1.000   0.100    90.0    0.00   0.010   0.015
C4         00.0    20.0     0.0
C5            0      12              20       0       1       1       0       1         1
CV         0.01    0.01   0.001   0.050   0.050               1    0.05
ED1           1     1.0     1.0     1.0     1.0    -1.0   1.000   1.000
ED2                 1.0     1.0   0.001             20.
ED4                0.05     0.0    0.00
ED1         908     1.0     1.0     1.0     1.0    -1.0   1.000   1.000       1
ED2                 1.0     1.0   0.001             20.
ED4                0.05     0.0    0.00
CC1    1    102     108     231     118     182
CC1    2     87     216     179     176     129
CC1    3    169     239      62     240      47
CC1    4    225     157      37      20       1
WDT         169   108.0     5.0   109.0
WDT         239   108.0     5.0   109.0
WDT          62   108.0     5.0   109.0
WDT         240   108.0     5.0   109.0
WDT          47   108.0     5.0   109.0
ENDGEO
DT        0.000
BC         6010    6010    6010    6010    6010    6010    6010    6010    6010
BC         6010    6010    6010
QC            1       0  200.00  1.5710   0.000  20.000   0.000
FC          908      10      0.      0.      0.      0.  1.5710
ENDSTEP
DT        0.500       0    1996      10
BC         6010    6010    6010    6010    6010    6010    6010    6010    6010
BC         6010    6010    6010
QC            1       0   30.00  1.5710   0.000  20.000   0.000
FC          908      10      0.      0.      0.      0.  1.5710
ENDSTEP
ENDDATA
```

Weir element types should be identified in ED lines. Values for Roughness class of weir elements should considered specially. When weirs are submerged, the back water effect is only taken into account by considering weirs as bottom roughness.

FC line should be added in the time step data block to define the continuity line for hydraulic structures. In the FC line, weir element type and the type of control structure are defined at first. If the control structure is a weir (type 10 in this case), the following 4 parameters are not in use. Only the last entry, which indicates the flow direction over the weir, is used.

If the weir overflow is calculated by RMA-10S, weir information should be entered at WDT lines in the control file. In this line, node number (supposed to be on the notional upstream side), elevation of weir crest, length of weir crest in the flow direction, and transition elevation should be entered sequentially. Information at WDT lines should be entered for each upstream or / and downstream corner node.

If the weir overflow is interpolated by the values entered in an external weir input file, file data line INCSTR should be added in the control file, followed by the name of the file. A sample of the weir input file and a short description of the identification lines are demonstrated below, just the same as in chapter 5.2.2.

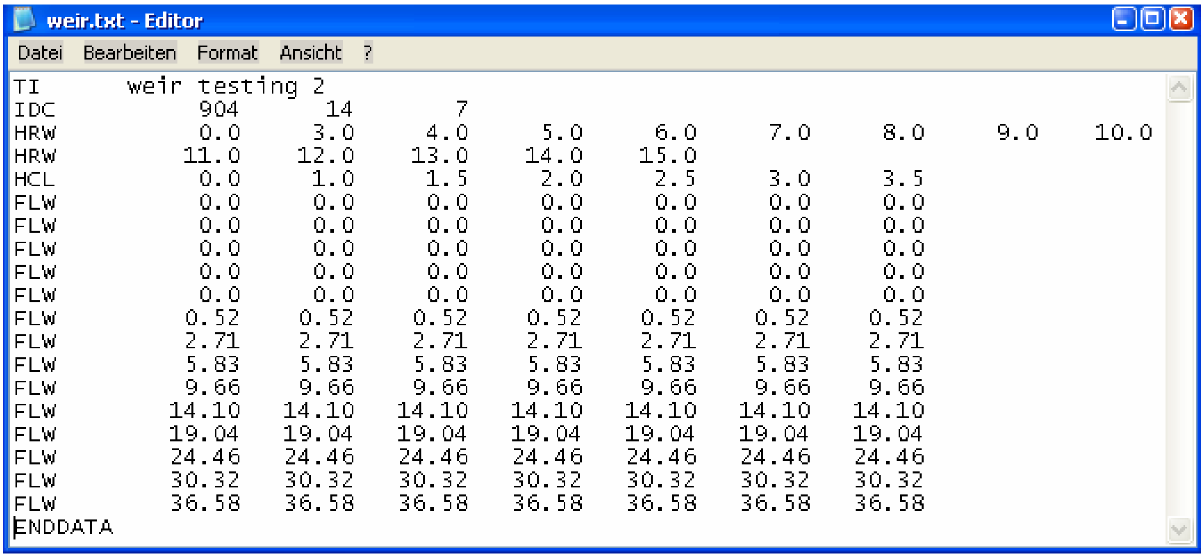

weir.txt - Editor

Datei Bearbeiten Format Ansicht ?

```
TI       weir testing 2
IDC          904      14       7
HRW          0.0     3.0     4.0     5.0     6.0     7.0     8.0     9.0    10.0
HRW         11.0    12.0    13.0    14.0    15.0
HCL          0.0     1.0     1.5     2.0     2.5     3.0     3.5
FLW          0.0     0.0     0.0     0.0     0.0     0.0     0.0
FLW          0.0     0.0     0.0     0.0     0.0     0.0     0.0
FLW          0.0     0.0     0.0     0.0     0.0     0.0     0.0
FLW          0.0     0.0     0.0     0.0     0.0     0.0     0.0
FLW          0.0     0.0     0.0     0.0     0.0     0.0     0.0
FLW         0.52    0.52    0.52    0.52    0.52    0.52    0.52
FLW         2.71    2.71    2.71    2.71    2.71    2.71    2.71
FLW         5.83    5.83    5.83    5.83    5.83    5.83    5.83
FLW         9.66    9.66    9.66    9.66    9.66    9.66    9.66
FLW        14.10   14.10   14.10   14.10   14.10   14.10   14.10
FLW        19.04   19.04   19.04   19.04   19.04   19.04   19.04
FLW        24.46   24.46   24.46   24.46   24.46   24.46   24.46
FLW        30.32   30.32   30.32   30.32   30.32   30.32   30.32
FLW        36.58   36.58   36.58   36.58   36.58   36.58   36.58
ENDDATA
```

TI: title for the file.

IDC: control structure definition data. In this line, element type, number of rows and columns for this element type should be defined sequentially.

HRW: upstream water surface elevations, maximum 9 entries per line, as many lines as required.

HCL: downstream water surface elevations, maximum 9 entries per line, as many lines as required.

FLW: flow for the corresponding row and column elevation defined earlier. Enter row wise (the whole line corresponds to the same upstream water surface elevation). One entry in the line is for the related column. Repeat as many lines as entries of upstream water surface elevations. Note that the values are in m^3/s per unit width, maximum 9 entries per line.

IDC, HRW, HCL and FLW should be repeated as many as weir element types defined in the model.

With all the changes and input into the model, the weir simulation should be able to be started.

Appendix III – Troubleshoot

Different problems have occurred at various stages during the work. Some of them appeared continuously. Therefore, some of the error messages appeared in the simulation window and the possible solutions are collected here.

ATTEMPT TO SET FLOW FOR NON-EXISTENT LINE 1
EXECUTION TERMINATED

It happens when the converted GEO file is used again with this version.
The possible cause would be that the continuity lines should be specified in RM1 file and then converted to GEO file or defined directly in GEO file.

ERROR UNDEFINED LEVEE DATA FOR NODE xxx

Weir data should be added at WDT lines in the control file.

REORDERING HAS TO BE DONE.
WIEVIELE KNOTEN WERDEN ALS STARTKNOTEN GEGEBEN?

It happens when the channel is generated by using “make_channel_0_2_1.exe” or “make_channel_0_2_2.exe” and used firstly as input for the simulation. The reason is not identified. It was only solved by retrying.

SUSPICIOUSLY LARGE NODE NUMBER 538976288OR LARGE ELEMENT NUMBER 538976288 DETECTED
EXECUTION TERMINATED

Ill defined network, most frequently happened when RM1 file is used as input geometry file.
Possible solution: load RM1 file in RMAGEN and save as binary GEO file, then use this GEO file as input geometry file.

UNSATISFIED ELIMINATION ERROR

It occurs especially while restarting or at the beginning of each time step. It is stated in RMA10 documentation from King (1993) that the possible cause would be ill defined network or ED lines. However, it might also come from the poor convergence or the format of the control file.

Possible solutions include every means to improve the convergence behaviour, e.g. increase the time step; sometime the highest water elevation should also be checked.

WARNING WEIR HEIGHT CLEARANCE LESS THAT 0.1 NODE xxxx CLEARANCE =

It is warning message to indicate that the weir crest is less than 0.1 m higher than the bottom elevation. The simulation is not influenced.